

# Chapter 7

## Chaos and Non-Linear Dynamics

By a deterministic systems of equations, we mean equations that given some initial conditions have a unique solution, like those of classical mechanics. In a deterministic system we will define *chaos* as aperiodic long-term behavior that exhibits sensitive dependence on initial conditions.

- Here “aperiodic behavior” means that phase space trajectories do not converge to a point or a periodic orbit, they are irregular and undergo topological mixing (discussed below).
- By “sensitive to initial conditions” we mean that trajectories that start nearby initially, separate exponentially fast. Defining  $\delta(t)$  as the difference between points on two such trajectories at time  $t$ , then this means that  $|\delta(t)| \propto \delta_0 e^{\lambda t}$  for some  $\lambda > 0$ , as depicted in Fig. 7.1.

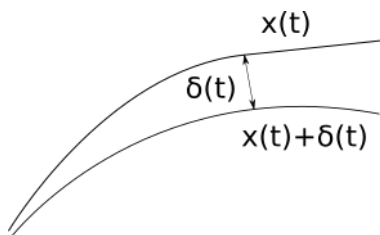


Figure 7.1: The difference in initial condition leads to different orbits. Their difference is given by  $\delta(t)$ , which grows exponentially with time.

This means that even though they are deterministic, chaotic systems are most often not predictable. In particular, there will always be a small difference  $\delta_0$  between the true and measured initial conditions for the system (from statistical or systematic measurement error), which grows exponentially to yield inaccurate predictions for predictions far enough in the future.

The sensitivity to initial conditions is important to chaos but does not itself differentiate from simple exponential growth, so the aperiodic behavior is also important. In the definition of this somewhat undescriptive phrase we include that the system should undergo *Topological Mixing*. This means that any points starting in a region (open set) of the phase space will evolve to overlap any other region of the phase space, so chaotic systems tend to explore a larger variety of regions of the phase space.<sup>1</sup>

## 7.1 Introduction to Chaos

We will now explore some properties of non-linear dynamical systems, including methods to characterize solutions, and the study of solutions with chaotic behavior.

### 7.1.1 Evolution of the system by first order differential equations

The dynamical system can be defined by a system of first order differential equations:

$$\begin{aligned}\dot{x}_1 &= f_1(x_1, \dots, x_n) \\ \dot{x}_2 &= f_2(x_1, \dots, x_n) \\ &\vdots \\ \dot{x}_n &= f_n(x_1, \dots, x_n)\end{aligned}\tag{7.1}$$

where the quantities  $x_i$ , for  $i \in \{1, \dots, n\}$ , are any variables that evolve in time, which could be coordinates, velocities, momenta, or other quantities. For our applications in this chapter we will often assume that the  $x_i$  equations are also chosen to be dimensionless, and the procedure for this type of conversion will be discussed further below.

**Example:** the Hamilton equations of motion are 1<sup>st</sup> order equations in the canonical variables, so they are an example of equation of the form in Eq. (7.1) with an even number of  $x_i$  variables.

#### Deterministic evolution from the existence and uniqueness theorem

Assume that we have a set of differential equations in the form in Eq. (7.1), which we can write in a shorthand as

$$\dot{\vec{x}} = \vec{f}(\vec{x}),\tag{7.2}$$

and that  $f_j$  and  $\frac{\partial f_j}{\partial x_i}$  (for  $i, j \in \{1, \dots, n\}$ ) are continuous in a connected region  $\mathbb{D} \in \mathbb{R}^n$ . Then if we have an initial condition  $\vec{x}(t=0) = \vec{x}_0 \in \mathbb{D}$ , then the theorem states that there exists a *unique* solution  $\vec{x} = \vec{x}(t)$  on some interval  $(-\tau, \tau)$  about  $t = 0$ . Time evolution in such a system is therefore deterministic from this existence and uniqueness theorem.

<sup>1</sup>For a dissipative chaotic system there are further restrictions on the choice of the open sets in this definition of topological mixing since it is otherwise obvious that we could pick a region that the system will not return to.

For this chapter the damped nonlinear oscillator will be a good to base our discussion. In the case of a pendulum with damping and a periodic driving force, its evolution is given by the equation of motion:

$$ml^2\ddot{\theta} + ml^2\gamma\dot{\theta} + mgl \sin(\theta) = A \cos(\omega_D t), \quad (7.3)$$

where  $\ell$  is the length of the pendulum,  $\theta$  is the oscillator angle,  $\gamma$  is the damping coefficient, and  $A \cos(\omega_D t)$  is the driving force. It is useful to turn this into a dimensionless equation. First we divide by  $mgl$  to make the third term dimensionless, defining

$$a \equiv \frac{A}{mgl}, \quad (7.4)$$

to give a dimensionless amplitude for the forcing term. This leaves

$$\frac{l}{g}\ddot{\theta} + \frac{\gamma l}{g}\dot{\theta} + \sin\theta = a \cos(\omega_D t). \quad (7.5)$$

Next to make the first term dimensionless we rescale the time derivatives so that they involve a dimensionless time  $t'$ , and change to a dimensionless frequency  $\omega'_D$  for the forcing term via

$$t' \equiv \sqrt{\frac{g}{l}}t, \quad \omega'_D \equiv \sqrt{\frac{l}{g}}\omega_D, \quad \dot{u} \equiv \frac{du}{dt} \Rightarrow \dot{u} \equiv \frac{du}{dt'}. \quad (7.6)$$

As indicated we also now let dots indicate derivatives with respect to the dimensionless time. Finally we define

$$\frac{1}{q} \equiv \sqrt{\frac{l}{g}}\gamma, \quad (7.7)$$

where  $q$  is the dimensionless quality factor for the damping term.

Dropping the newly added primes, our final differential equation is now fully dimensionless:

$$\ddot{\theta} + \frac{1}{q}\dot{\theta} + \sin(\theta) = a \cos(\omega_D t) \quad (7.8)$$

Here  $a$ ,  $q$ , and  $\omega_D$  are all dimensionless constants. We can convert this into 1<sup>st</sup> order form by defining  $\varphi \equiv \omega_D t$  to get rid of the explicit time dependence in the forcing term, and  $\dot{\theta} \equiv \omega$  to eliminate the double time derivatives. This gives the system of three equations that are in the form in Eq. (7.1) with  $\vec{x} = (\theta, \omega, \varphi)$ :

$$\begin{aligned} \dot{\theta} &= \omega, \\ \dot{\omega} &= -\frac{1}{q}\omega - \sin(\theta) + a \cos(\varphi), \\ \dot{\varphi} &= \omega_D. \end{aligned} \quad (7.9)$$

### 7.1.2 Evolution of Phase Space

#### Phase space trajectories never cross

From the uniqueness theorem, phase space trajectories never cross. To prove this, note that any point  $\vec{x}(t)$  on a trajectory could be used as an initial condition for a new trajectory. Since a point can only be part of one single trajectory, no crossings can occur.

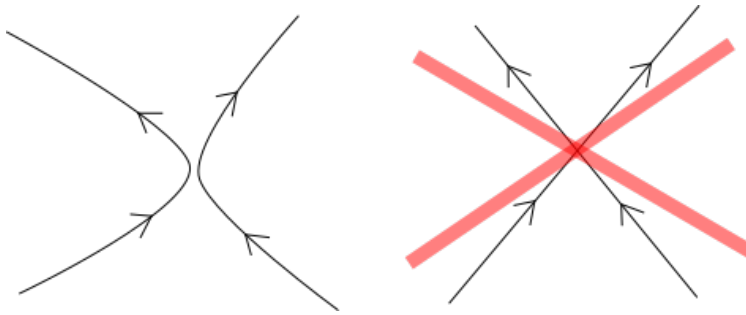


Figure 7.2: By the uniqueness theorem, no two trajectories can cross, only come arbitrarily close.

#### Evolution of phase space volume

The phase space volume is given by:

$$\mathcal{V} = \int_{\mathcal{V}} \prod_{j=1}^n dx_j \quad (7.10)$$

Recall that for Hamiltonian systems, canonical transformations do not change volume elements. If we view this transformation as a solution for motion (via the H-J equation), then it is clear that the motion generated by a Hamiltonian preserves the volume, so  $\dot{\mathcal{V}} = 0$ .

What happens with damping/friction (which is not in our Hamiltonian formalism)? To determine the answer we can exploit an analogy with our results for changes in volume for fluids:

$$\begin{aligned} \dot{\mathbf{x}} = \mathbf{v}(\mathbf{x}) &\Leftrightarrow \dot{\vec{x}} = \vec{f}(\vec{x}), \\ \dot{V} = \int dV \nabla \cdot \mathbf{v} &\Rightarrow \dot{\mathcal{V}} = \int d\mathcal{V} \nabla \cdot \vec{f}. \end{aligned} \quad (7.11)$$

where in the context of a general nonlinear system,  $\nabla$  refers to derivatives with respect to  $\vec{x}$ . Thus we see that  $\nabla \cdot \vec{f}$  determines the change to a volume of our phase space variables. For this reason we define  $\nabla \cdot \vec{f} = 0$  as a *conservative system* (whether or not a general Hamiltonian exists), while  $\nabla \cdot \vec{f} < 0$  is a *dissipative system* where the phase space volume shrinks.

For our damped nonlinear driven oscillator example we have:

$$\nabla \cdot \vec{f} = \frac{\partial \omega}{\partial \theta} + \frac{\partial}{\partial \omega} \left( -\frac{1}{q} \omega - \sin(\theta) + a \cos(\varphi) \right) + \frac{\partial \omega_D}{\partial \varphi} = -\frac{1}{q} < 0, \quad (7.12)$$

as expected for a dissipative system.

For the special case of  $q \rightarrow \infty$  and  $a = 0$  (undamped and undriven system), then:

$$\dot{\theta} = \omega, \quad \text{and} \quad \dot{\omega} = -\sin(\theta). \quad (7.13)$$

The corresponding trajectories in phase space are illustrated below:

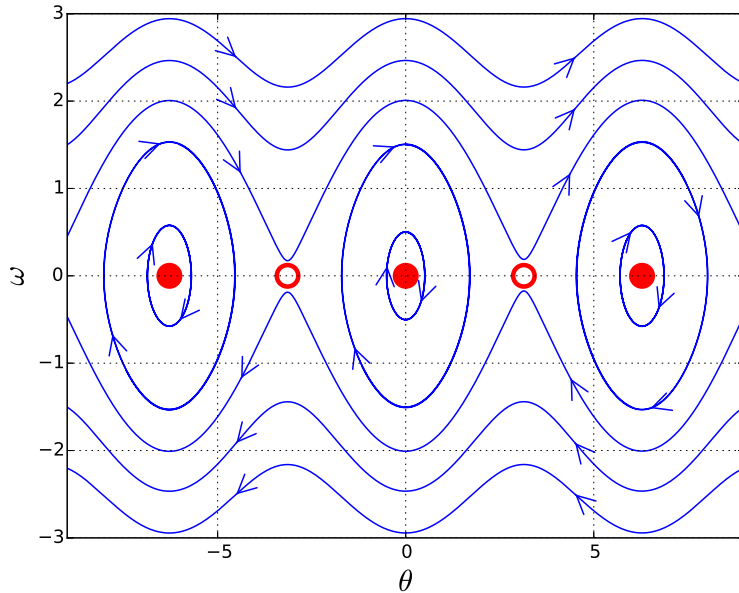


Figure 7.3: Phase space picture of the undamped, unforced oscillator. Filled circles are the stable fixed points and empty circles are the saddle points which are fixed points that are unstable in one direction and stable in another.

### 7.1.3 Fixed Points

Of particular interest in a system are its *fixed points*,  $\vec{x}^*$ , defined as the locations where

$$\vec{f}(\vec{x}^*) = 0. \quad (7.14)$$

At these points the state of the system is constant throughout time. Depending on the behavior of the trajectories nearby the fixed point they can be characterized as:

- *Stable* - nearby trajectories approach the stable point

- *Unstable* - nearby trajectories move away from the fixed point
- *Saddle Point* - in different directions trajectories can either approach or move away

For the undriven, undamped oscillator (Eq.(7.13)), the system has fixed points for  $\omega = 0$  and  $\theta = n\pi$  for any integer  $n$ . For this pendulum, the fixed point at the bottom  $\theta = 2\pi n$  is stable, while the fixed point at the top is unstable  $\theta = \pi(2n + 1)$ , as shown in Fig. 7.3. Note that this fixed point at the top is not a crossing trajectory because we can only get to this point if  $E = 0$  exactly, and in that case the trajectory would stop at this fixed point. Any small perturbation knocks it off the unstable point at the top and determines which way it goes.

If there is dissipation, then all trajectories in the neighborhood of a stable fixed point converge upon it, so this region is called the *basin of attraction* and the fixed point is an *attractor*; energy dissipates as motion decays to the attractor. In our example it occurs if  $q$  is finite, and the basins of attraction in this case are diagonal strips in phase space. The result for two trajectories in phase space are shown below.

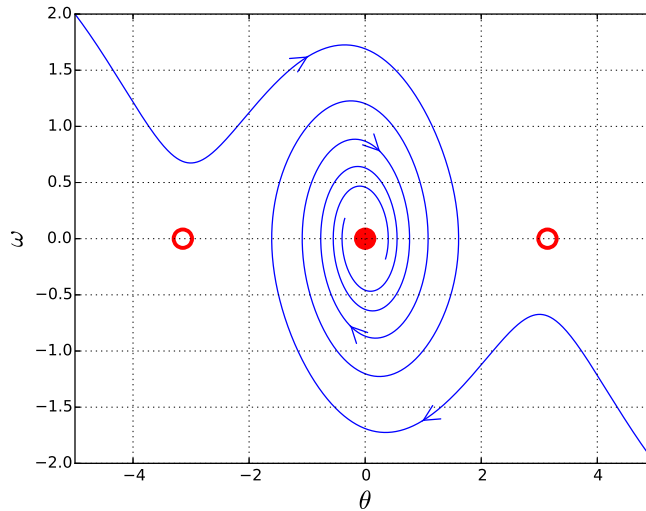


Figure 7.4: With finite damping ( $q = 5$ ) in our oscillator example the trajectories converge to the stable fixed points of the system with spiraling motion.

#### Conditions for chaotic behavior

In general, two necessary conditions for chaos are:

- The equations of motion must be nonlinear. (For linear systems we already know the solutions, which are exponential or oscillating and hence not chaotic.)

- There must be at least 3 variables, so if  $i \in \{1, \dots, n\}$ , then  $n \geq 3$ . (We will see why this is necessary later.)

In our non-linear damped oscillator example, now including a non-zero forcing term gives rise to a wider range of qualitative behaviors. In particular for certain values of  $(a, q, \omega_D)$  the system can be chaotic.

If we start instead with the linearized version of the forced damped oscillator then we have:

$$\dot{\omega} = -\frac{1}{q}\omega - \theta + a \cos(\varphi) \quad (7.15)$$

For this case the solution, which is non-chaotic, are well known and often studied in elementary courses in classical mechanics or waves. The general solutions come in three cases, underdamped ( $q > 1/2$ ), critically damped ( $q = 1/2$ ), or overdamped ( $q < 1/2$ ). For example the general underdamped solution is given by:

$$\theta(t) = Be^{-\frac{t}{2q}} \cos\left(t\sqrt{1 - \frac{1}{4q^2}} + \varphi_0\right) + \frac{a}{\omega_D \sqrt{q^{-2} + (\omega_D^{-1} - \omega_D)^2}} \cos(\omega_D t - \delta), \quad (7.16)$$

where  $\tan(\delta) = \omega_D/(q - q\omega_D^2)$ , and  $B$  and  $\varphi_0$  are constants that are determined by the initial conditions. The first term in Eq. (7.16) is the transient that decays away exponentially, whereas the second term describes the steady state forced motion (whose amplitude exhibits resonant behavior at  $\omega_D = 1$ ).

A projection of the trajectories into the 2-dimensional  $\theta-\omega$  plane, as shown in Fig. 7.5 shows that they converge onto ellipses after many cycles. This does not break the uniqueness theorem since  $\varphi = \omega_D t$  is increasing, so the trajectory never crosses itself when all three variables are plotted. If restrict  $\varphi \in [0, 2\pi]$  then the trajectory converges to a closed orbit. Note that the nonlinear forcing term  $\cos(\varphi)$  is important to ensure that this closed orbit is an isolated stable endpoint for the motion.

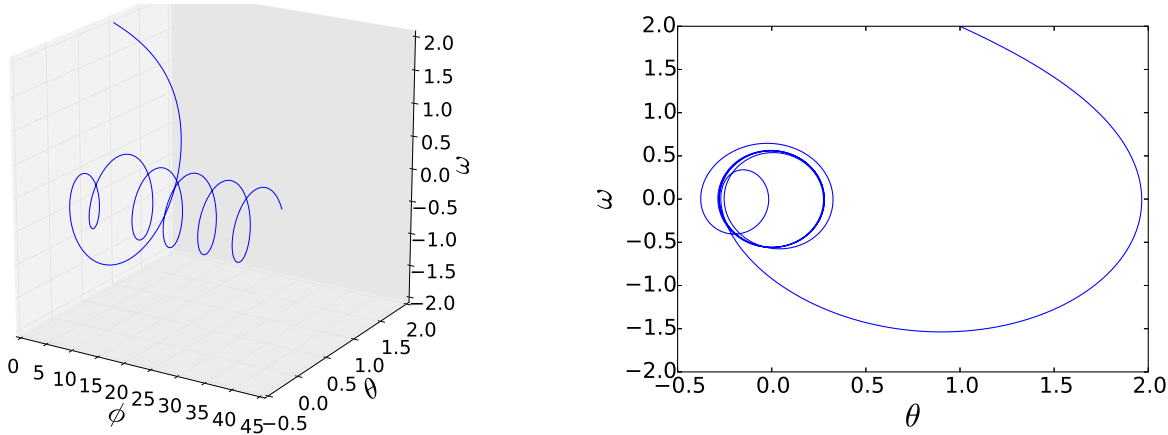


Figure 7.5: Although the  $\theta - \omega$  projection of the system shows crossings, which would seem to violate the uniqueness theorem, plotting the 3 variables we see that no crossing occurs, and uniqueness is preserved. In the projection plot we also clearly see the system evolving to a closed orbit.

An attractor that is a closed orbit rather than a single point is called a *limit cycle*.

### 7.1.4 Picturing Trajectories in Phase Space

#### 2-dim projections

To solve the full nonlinear damped forced oscillator, described by the solution to Eq. (7.9), we use a computer. Note that we can examine chaos and sensitivity to initial conditions on a computer since the various phenomena, including the exponential growth of differences due to chosen initial conditions, occur much before the differences due to truncation errors associated with machine precision take over. In order to give a taste of what chaos looks like, we will first simply examine some of the results especially as applied to the nonlinear oscillator.

One way to see chaos is to do a projection of trajectories in the full  $n$ -dimensional space of variables to a lower dimension (usually down to 2 dimensions so we can plot results in a plane). For the nonlinear oscillator, this is typically the  $\theta-\omega$  plane where we project away  $\varphi$  (as in the right most images of Fig. 7.5). For chaotic motion this projection yields a two dimensional picture which in general gets quite messy, with the trajectory filling out a large area of the plane.

#### Poincaré Section (Poincaré Map)

To simplify things further we can use a Poincaré section (also called a Poincaré map). Here we sample the trajectory periodically in  $\varphi$  say when  $\varphi = 2\pi n$  which is the periodicity of  $\cos \varphi$  for our example, and plot only these values  $(\theta_n, \omega_n)$  in the  $\theta-\omega$  plane. The results we

track are then much like what we would observe by looking at the system with a stroboscope. For creating the Poincaré section of any such system, we wait until the transients die out.

For the nonlinear oscillator, this might be at  $\varphi = 2\pi n$  for integer  $n$ , yielding a sampling frequency of exactly  $\omega_D$ , so the map is a plot of only these values  $(\theta_n, \omega_n)$ . For example, we could take  $\omega_D = \frac{2}{3}$  and  $q = 2$  while varying  $a$  as in Fig. 7.6; where we have waited for 30 cycles to ensure that the transients have died out.

In figure Fig. 7.6 we show both 2-dimensional phase portraits and Poincaré maps for various values of  $a$ . As  $a$  increases the plots show singly periodic long term behavior ( $a = 0.9$ ), to doubly periodic ( $a = 1.07$ ), to chaotic ( $a = 1.19$ ), and finally to periodic again occurring amidst neighboring chaos ( $a = 1.35$ ).

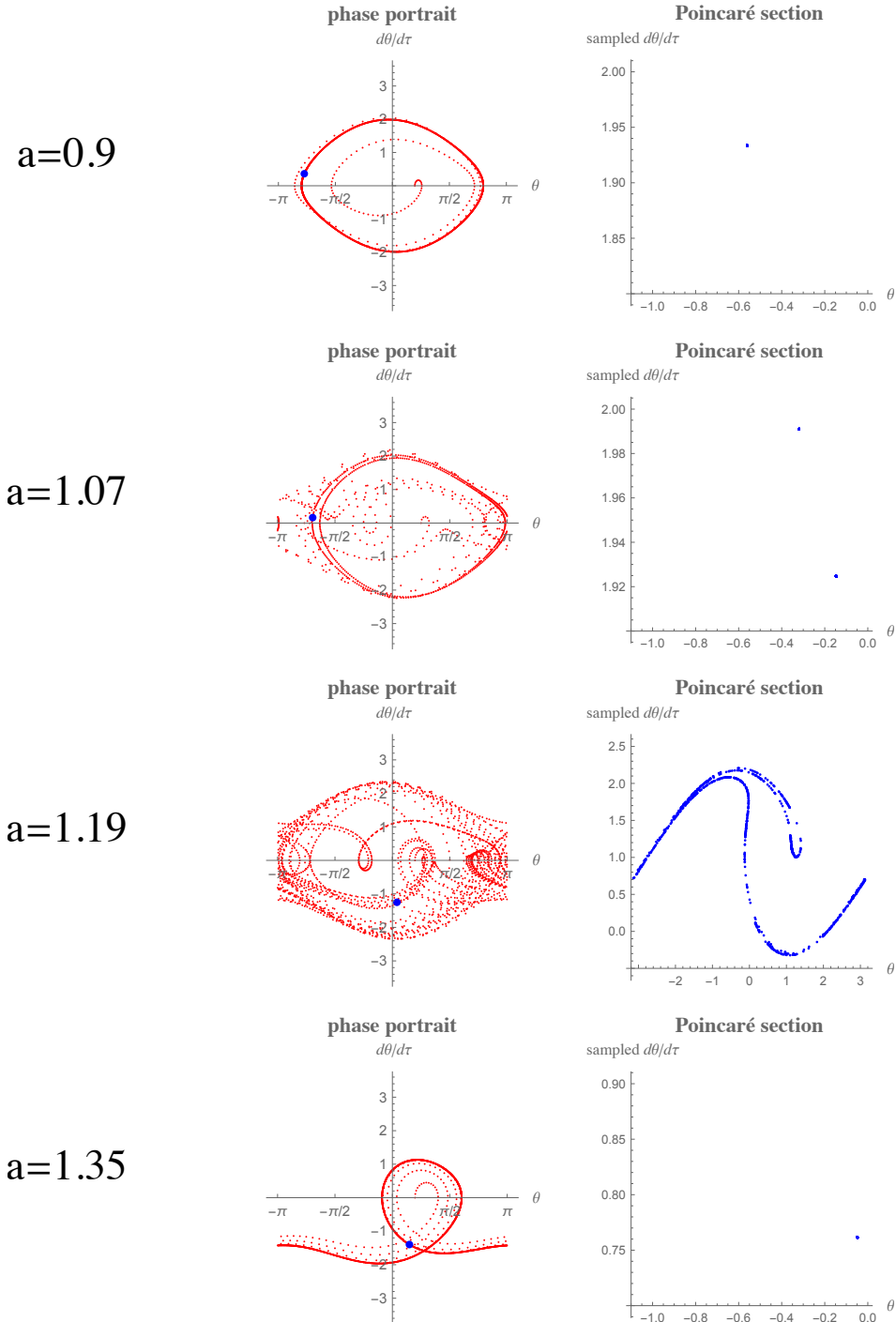


Figure 7.6: Phase portraits and Poincaré sections for the nonlinear driven damped oscillator with  $\omega_D = 2/3$ ,  $q = 2$ , and various values of  $a$ . The plots show singly periodic, doubly periodic, chaotic, and singly periodic behavior respectively. (Plots generated with the Mathematica demonstration package, Chaotic Motion of a Damped Driven Pendulum, by Nasser Abbasi.)

### Bifurcation Map

Yet another way is through a bifurcation diagram, which takes the Poincaré map results but plots one of the variables against one of the parameters of the system. This plot allows us to see the transitions between different behaviors, in particular a change in the fixed points of the system. For the nonlinear oscillator, this could be a plot of  $\omega$  against  $a$ , as shown in Fig. 7.7.

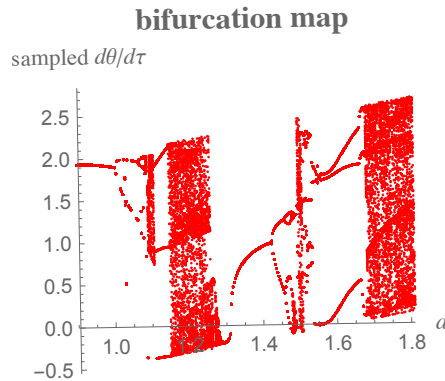


Figure 7.7: For the Driven damped nonlinear oscillator, plot of  $\omega = \dot{\theta}$  values obtained from the Poincaré map as a function of  $a$  with  $Q = 2$  and  $\omega_D = 2/3$  fixed. This bifurcation plot show the qualitative transitions of the system, such as where period doubling/bifurcation occurs, and where chaos starts. (Plot generated with the Mathematica demonstration package, Chaotic Motion of a Damped Driven Pendulum, by Nasser Abbasi.)

There are a few notable features in this bifurcation plot which we summarize in the following table:

$a$	Features
1.0	only a single $\omega$
1.07	two values of $\omega$ from the same initial conditions ( <i>period doubling</i> )
1.15-1.28	mostly chaos (some periodic windows)
1.35	periodic again

Other parameter choices also lead to qualitatively similar bifurcation plots, with quantitatively different windows of periodic behavior and chaos. We can also obtain bifurcation plots which exhibit both periodic and chaotic windows by plotting  $\omega$  against other parameters of the system, such as  $\omega_D$ .

## 7.2 Bifurcations

In our analysis of the nonlinear damped forced oscillator, we took snapshots  $(\theta_n, \omega_n)$  at  $\varphi = 2\pi n$  for integer  $n$  to form the Poincaré map. When we changed the driving amplitude  $a$ , there were qualitative changes to the  $(\theta, \omega)$  projected trajectories (which are also generally called phase portraits) captured by the Poincaré map results. In particular, we observed period doubling at certain values of  $a$ ; period doubling is a particular example of a bifurcation (Fig.(7.7)).

A simple example of an abrupt change is when the existence/type of fixed points changes with the system's parameters (or limit cycles, attractors, or so on) abruptly changes. These changes are generally known as *bifurcations*. Since bifurcations already occur in 1-dimensional systems, so we will start by studying these systems. We will later on find out that many examples of bifurcations in higher-dimensions are simple generalizations of the 1D case.

For a 1-dimensional system we study the equation:

$$\dot{x} = f(x) \tag{7.17}$$

Trajectories in 1 dimension are pretty simple, we either have flow to a finite fixed point  $x \rightarrow x^*$  or a divergence to  $x \rightarrow \pm\infty$ .

**Example:** The system  $\dot{x} = x^2 - 1$ , pictured in Fig. 7.8, has a stable fixed point at  $x^* = -1$  and an unstable fixed point at  $x^* = 1$ . For one dimension the motion is simple enough that we can determine whether fixed points are stable or unstable simply from this picture. Imagine a particle moving on the  $x$ -axis. For  $x < -1$  the red curve of  $x^2 - 1$  is above the  $x$ -axis, so  $\dot{x} > 0$  and the particle moves to the right, as indicated by the blue arrow. For  $-1 < x < 1$  the red curve is below,  $\dot{x} < 0$ , and the particle moves to the left. For  $x > 1$  the curve is again above,  $\dot{x} > 0$  and the particle moves to the right. The left point is stable since the particle always moves towards it, while the right point is unstable and the particle moves away from it.

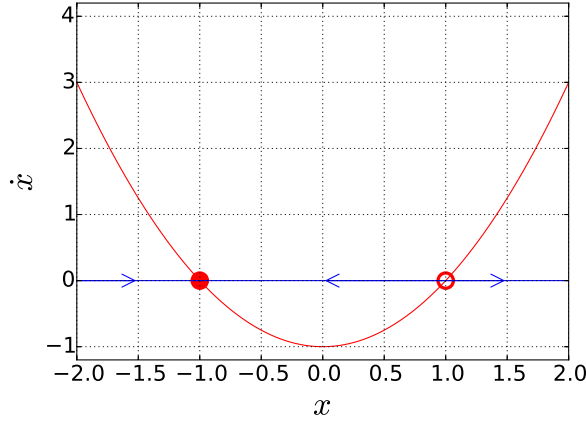


Figure 7.8: In this system there are two fixed points, one stable (represented by a full circle) and one unstable (represented by the empty circle)

Stability can also be determined by linearizing about a fixed point. Although this is overkill for one variable, the general method remains applicable for analyzing situations with more variables, so its useful to discuss it here. Using  $x = x^* + \eta$  and expanding to  $\mathcal{O}(\eta)$ , then  $\dot{\eta} = \dot{x} = x^2 - 1 \approx 2x^*\eta$ , so for  $x^* = -1$ , then  $\dot{\eta} = -2\eta$  which decays according to  $\eta \propto e^{-2t}$  making the fixed point stable, while for  $x^* = 1$ , then  $\dot{\eta} = 2\eta$  which grows according to  $\eta \propto e^{2t}$  and the fixed point is unstable.

To find the stability of fixed points in multiple dimensions, we would similarly set  $\vec{x} = \vec{x}^* + \vec{\eta}$  and expand, giving a linearized system of equations after dropping  $\mathcal{O}(\eta^2)$  terms:

$$\dot{\vec{\eta}} = M\vec{\eta} \quad (7.18)$$

Here  $M$  is a  $n \times n$  matrix, whose eigenvalues and eigenvectors give us the solutions near the fixed point, of the form  $\vec{\eta} = \vec{a}e^{\lambda t}$ . We will come back later on to discuss higher dimensional fixed points in much more detail.

First we will categorize several types of bifurcations in one dimension, by considering the equation

$$\dot{x} = f(x, r), \quad (7.19)$$

where  $r$  is a parameter that we vary. The fixed points  $x^*$  of  $f(x, r)$  are functions of  $r$ , and drawing them in the  $r - x$ -plane gives a *bifurcation diagram*.

### 7.2.1 Saddle-Node Bifurcation

A saddle-node bifurcation is the basic mechanism by which fixed points are created and destroyed. As we vary  $r$  two fixed points can either appear or disappear (one stable and one unstable).

**Example:** Consider the equation

$$\dot{x} = r + x^2, \quad (7.20)$$

which exhibits a saddle-node bifurcation at  $r = 0$ . The two fixed points disappear as we increase  $r$  from negative to positive values, as shown in the images below.

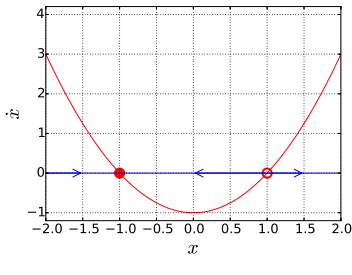


Figure 7.9: Two fixed points, one stable and one unstable exist for  $r < 0$

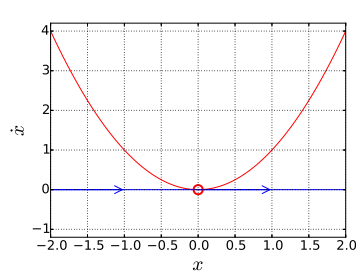


Figure 7.10: A single semi-stable point exists for  $r = 0$

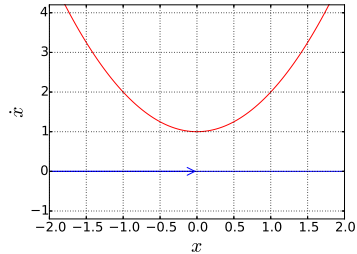


Figure 7.11: No fixed points occur for  $r > 0$

This saddle-node bifurcation transition can be best pictured by the bifurcation diagram in Fig. 7.12 below, where the full lines correspond to the stable fixed points and the dashed lines the unstable ones.

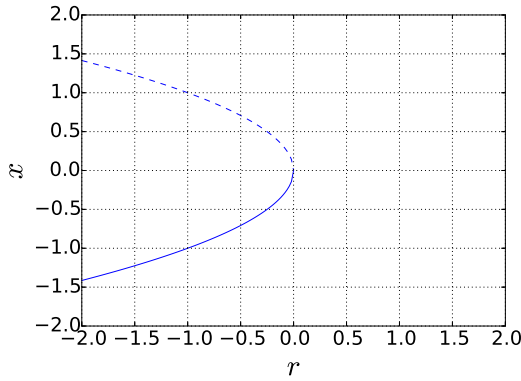


Figure 7.12: Bifurcation diagram for the system  $\dot{x} = r + x^2$

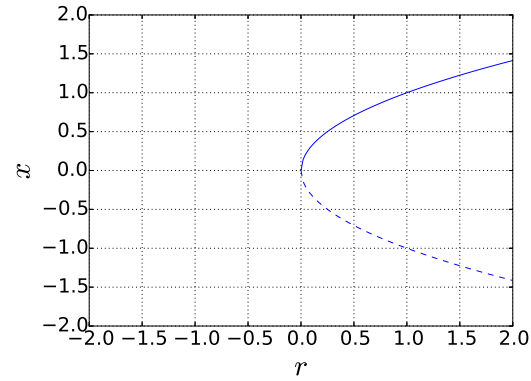


Figure 7.13: Bifurcation diagram for the system  $\dot{x} = r - x^2$

For the analogous equation  $\dot{x} = r - x^2$  we can obtain the results by interchanging  $x \rightarrow -x$  and  $r \rightarrow -r$ . This gives the bifurcation diagram shown in Fig. 7.13.

**Example:** Some flow equations like

$$\dot{x} = r - x - e^{-x} = f(x, r) \quad (7.21)$$

are hard to solve analytically for the fixed points, which are given by the transcendental equation

$$r - x^* = e^{-x^*} \quad (7.22)$$

Here a graphical approach suffices, where we separately plot  $r - x$  and  $e^{-x}$  and look for intersections of the curves to provide the position of the fixed points, as displayed in Fig. 7.14.

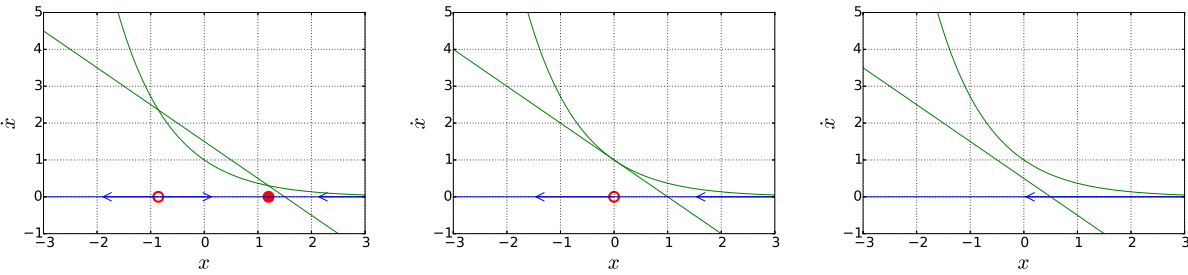


Figure 7.14: Fixed points of the system correspond to the intersections of the curves  $e^{-x}$  and  $r - x$  for  $r = 1.5$ ,  $r = 1.0$ ,  $r = 0.5$  respectively. As  $r$  is varied the position of the fixed points varies and a Saddle-Node Bifurcation occurs.

Examining which curve is larger also determines the direction of the one-dimensional flow, and hence the stability of the fixed points.

Here the bifurcation occurs at  $r = r_C$ , when the two curves are tangential and hence only touch once:

$$\left. \frac{\partial f}{\partial x} \right|_{x=x^*, r=r_C} = 0 \quad (7.23)$$

This gives  $-1 = -\exp(-x^*)$  so  $x^*(r_C) = 0$ . Plugging  $x^* = 0$  into Eq. (7.22) we find that  $r_C = 1$ .

By a simple generalization, we can argue that the quadratic examples  $\dot{x} = r \pm x^2$  are representative of all saddle-node bifurcations. Taylor expanding  $f(x, r)$  near the bifurcation point and fixed point we have

$$\begin{aligned} \dot{x} &= f(x, r) = f(x^*, r_C) + (x - x^*) \left. \frac{\partial f}{\partial x} \right|_{x^*, r_C} + (r - r_C) \left. \frac{\partial f}{\partial r} \right|_{x^*, r_C} + \frac{(x - x^*)^2}{2} \left. \frac{\partial^2 f}{\partial x^2} \right|_{x^*, r_C} + \dots \\ &= a(r - r_C) + b(x - x^*)^2 + \dots, \end{aligned} \quad (7.24)$$

where we have kept the first non-trivial dependence on  $r$  and  $x$  (noting that the partial derivatives are simply some constants  $a$  and  $b$ ), and two terms have vanished due to the

fixed point and by the tangential bifurcation conditions:

$$f(x^*; r_C) = 0 \quad \text{and} \quad \left. \frac{\partial f}{\partial x} \right|_{x=x^*, r=r_C} = 0. \quad (7.25)$$

Thus  $\dot{x} = r \pm x^2$  is the normal form of a saddle-node bifurcation. This can be determined explicitly from Eq. (7.24) by making the change of variable  $r' = a(r - r_C)$  and  $x' = \sqrt{|b|}(x - x^*)$  to obtain  $\dot{x}' = r' \pm x'^2$  where the  $\pm$  sign is determined by the sign of  $b$ .

### 7.2.2 Transcritical Bifurcation

In a transcritical bifurcation a fixed point exists for all values of the parameter, but changes its stability as the parameter is varied.

**Example:** Consider the equation

$$\dot{x} = x(r - x). \quad (7.26)$$

Here there are fixed points at  $x^* = 0$  and  $x^* = r$ . These fixed points change their stability at  $r = 0$  but never disappears as illustrated graphically in Fig. 7.15.

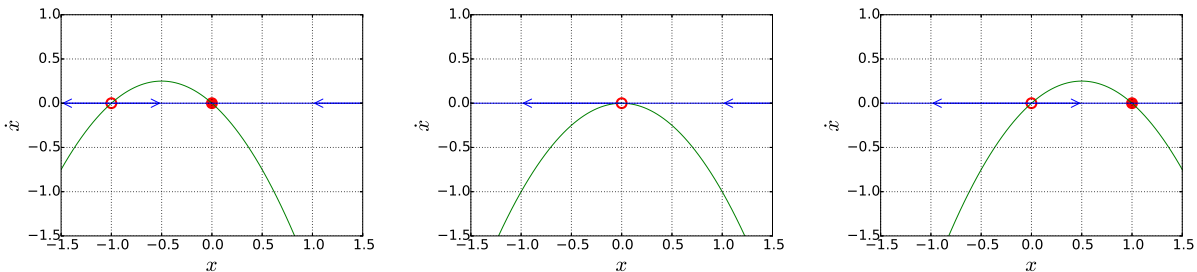


Figure 7.15: Analysis of  $\dot{x} = x(r - x)$  for  $r = -1$ ,  $r = 0$  and  $r = 1$  respectively. As  $r$  changes the same type of fixed points remain, but the stability of the fixed points is swapped.

This gives us the following bifurcation diagram:

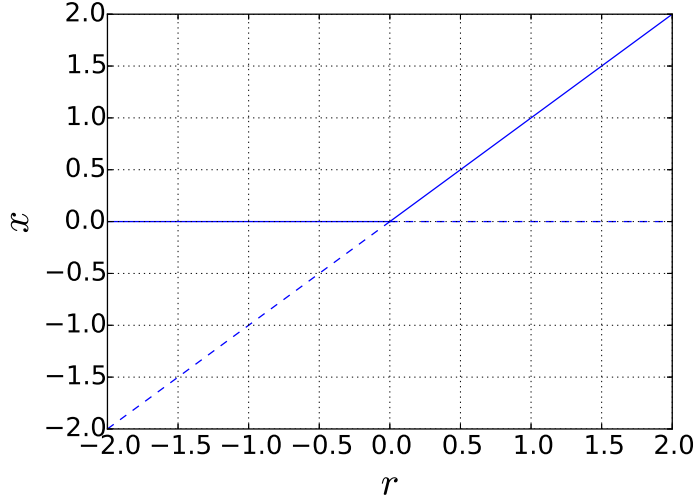


Figure 7.16: Bifurcation diagram for the system  $\dot{x} = x(r - x)$  which plots the position of the fixed points, with a full and dashed line for the stable and unstable points respectively. Here the transcritical bifurcation at  $r = 0$  becomes clear.

In fact, the equation “ $\dot{x} = x(r - x)$ ” is the normal form of a transcritical bifurcation obtained by expanding in a Taylor series near  $x = x^*$  and  $r = r_C$ .

**Example:** Lets consider an example with physical content, namely a model for the threshold behavior of a laser. This can be modeled as:

$$\begin{aligned}\dot{n} &= GnN - Kn, \\ \dot{N} &= -GnN - fN + p.\end{aligned}\tag{7.27}$$

where the variables are  $N$  the number of excited atoms and  $n$  the number of laser photons. The constant parameters include,  $f$  for the term governing the spontaneous emission decay rate,  $G$  for the stimulated emission gain coefficient,  $K$  as the photon loss rate, and  $p$  as the pump strength. Since there are two equations this is in general a two dimensional system (which we will discuss how to analyze shortly). Here to make the equation one dimensional we will assume rapid relaxation so that  $\dot{N} \approx 0$ , this allows us to solve for  $N(t)$  from the second equation in Eq. (7.27) to give

$$N(t) = \frac{p}{Gn(t) + f}.\tag{7.28}$$

Plugging this back into the first equation in Eq. (7.27) then gives

$$\dot{n} = \frac{n}{Gn + f} [pG - K(Gn + f)] \approx n(r - x) + O(n^3)\tag{7.29}$$

Expanding this result near  $n = 0$  we find

$$\dot{n} = n(r - bn) + O(n^3) \quad (7.30)$$

where the constant coefficients are

$$r \equiv \frac{pG}{f} - K, \quad b \equiv \frac{G^2 p}{f^2}. \quad (7.31)$$

Only  $n > 0$  makes sense, so the critical parameter value is when  $r = 0$ , or when the pump strength  $p = \frac{Kf}{G}$ . For larger values of  $p$  this lamp turns into a laser, with a fixed point at a non-zero  $n = r$  as illustrated in Figs. 7.17 and 7.18. The fixed point for  $p > \frac{Kf}{G}$  indicates the coherent laser action.

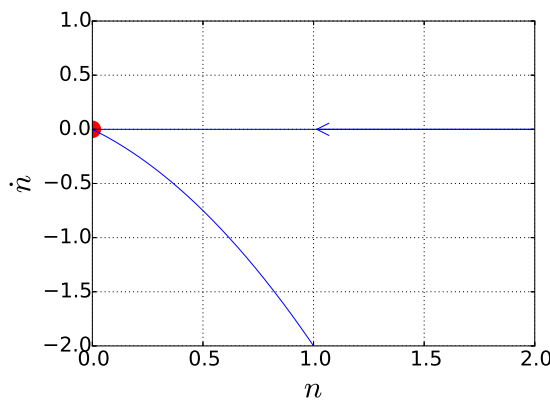


Figure 7.17: When  $p < Kf/G$ , the only stable point is when there are no photons.

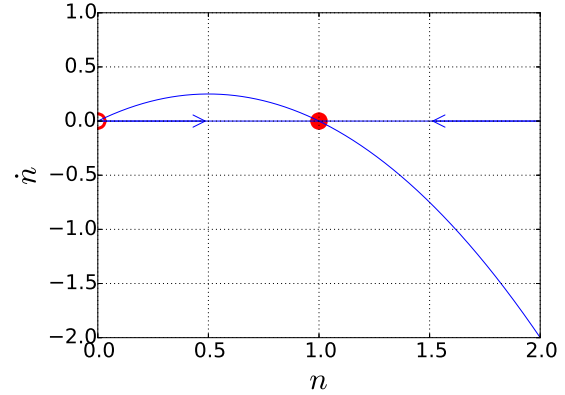


Figure 7.18: When  $p > Kf/G$ , the stable point of the system is with a non-zero number of laser photons.

### 7.2.3 Supercritical Pitchfork Bifurcation

A supercritical pitchfork bifurcation is a type of bifurcation common in problems with symmetries such that fixed points appear or disappear in pairs. In particular, as the parameter is varied, one fixed point is always present but changes from being stable to being unstable at the same place where two stable fixed points appear.

**Example:** The normal form for this type of bifurcation is

$$\dot{x} = rx - x^3. \quad (7.32)$$

This equation is invariant under  $x \leftrightarrow -x$ , so the fixed point  $x^* = 0$  is always present. On the other hand, the fixed points at  $x^* = \pm\sqrt{r}$  only appear when  $r$  crosses from negative to positive values. The different cases that occur as we change  $r$  are plotted in Fig. 7.19.

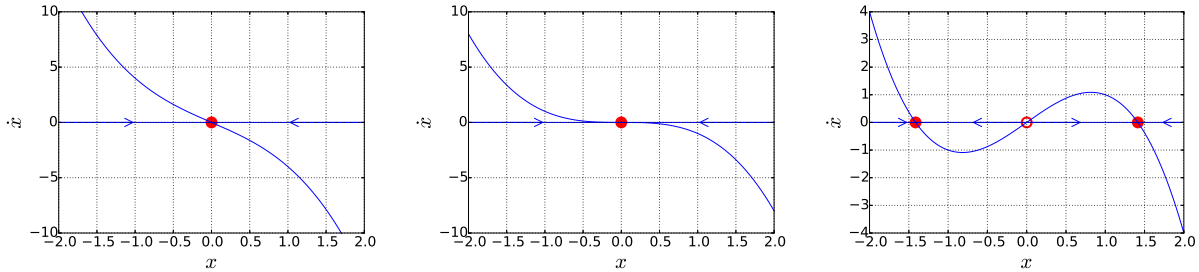


Figure 7.19: Plots of  $\dot{x} = rx - x^3$  for  $r = -2, 0, +2$  respectively. When  $r$  becomes positive the fixed point at  $x = 0$  loses its stability, and two new stable fixed points appear in the system.

This gives rise to the following bifurcation diagram:

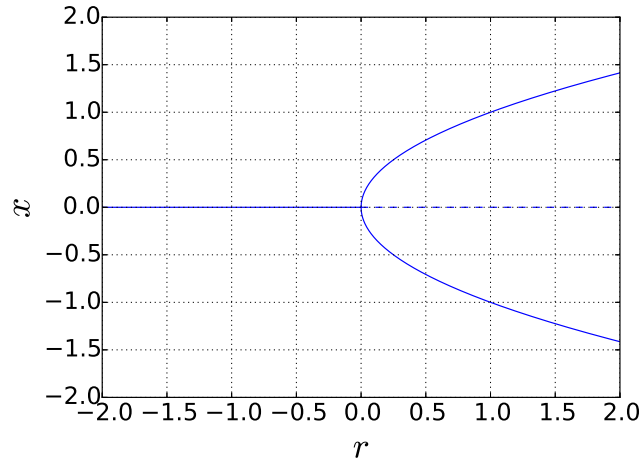


Figure 7.20: Diagram for the supercritical pitchfork bifurcation. The stability of the fixed point at  $x = 0$  changes while two new stable points appear.

### 7.2.4 Subcritical pitchfork bifurcation

A subcritical pitchfork bifurcation essentially the opposite of a supercritical pitchfork bifurcation in that if the parameter is varied, one fixed point that is always present changes from unstable to stable, while two unstable fixed points appear.

**Example** As an example consider the normal form

$$\dot{x} = rx + x^3, \quad (7.33)$$

which again has a  $x \rightarrow -x$  symmetry. Here the cubic term is destabilizing, so this exhibits a subcritical pitchfork bifurcation as depicted in Fig. 7.21.

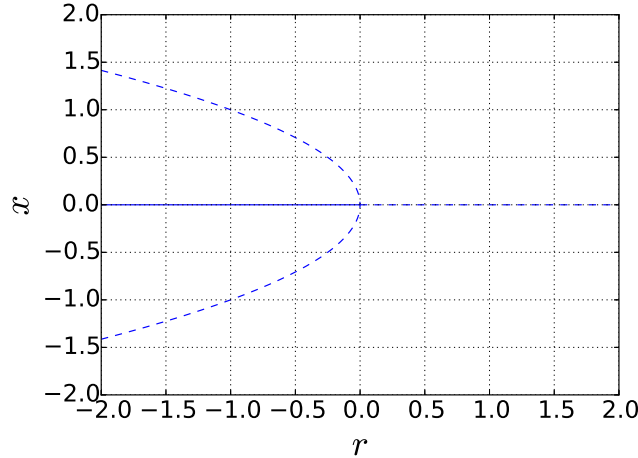


Figure 7.21: Bifurcation Diagram for the Subcritical Bifurcation  $\dot{x} = rx + x^3$ . Here there is a change in the stability of the fixed point at  $x = 0$  and the appearance of two new fixed points at  $x = \pm\sqrt{-r}$  as  $r$  becomes negative.

It is interesting to consider what happens if we add a higher order stabilizing term, such as in the equation

$$\dot{x} = rx + x^3 - x^5. \quad (7.34)$$

This equation supports five real solutions for a finite range of  $r$  values. This system supports hysteresis as we increase and decrease  $r$  as illustrated in Fig. 7.22. We can imagine a path where we start with a particle at  $x = 0$  and  $r = -0.2$  and then slowly increase  $r$ . When we get to  $r = 0$  the  $x = 0$  fixed point becomes unstable and a small perturbation will push the particle to another branch, such as that at  $x > 0$ . Increasing  $r$  further the particle travels up this branch. If we then start to decrease  $r$ , the particle will travel back down this same branch, and continue on it even below  $r = 0$ , and thus not following the same path. Then suddenly at the critical  $r_C < 0$  where there is a saddle-node bifurcation, the particle will again lose its stability and will jump back down to  $x = 0$ , after which the process can be repeated.

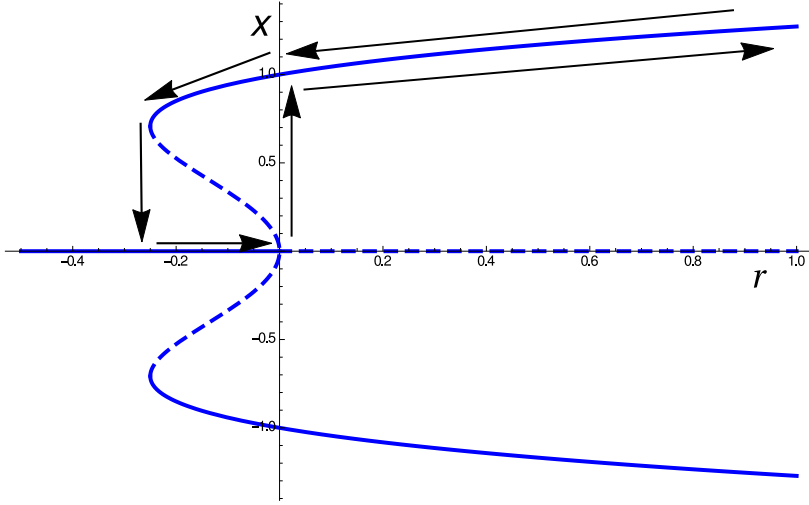


Figure 7.22: Bifurcation Diagram of the system  $\dot{x} = rx + x^3 - x^5$ . The arrows show the motion of the system as we increase and decrease  $r$ ; it undergoes hysteresis.

**Example:** Lets consider a bead on a rotating hoop with friction, described by the equation of motion:

$$ma\ddot{\theta} + b\dot{\theta} = m \sin \theta (a\omega^2 \cos \theta - g). \quad (7.35)$$

Here  $\theta$  is the angle of the bead of mass  $m$  from the bottom of the hoop,  $a$  is the radius of the hoop,  $\omega$  is the constant angular velocity for the rotation of the hoop (about an axis through the center of the hoop and two points on the hoop), and  $g$  is the coefficient of gravity. Once again to turn this into a one-dimensional problem we consider the overdamped solution. Overdamping means we can take  $ma\ddot{\theta} \rightarrow 0$ . The fixed points are then  $\theta^* = 0$  which changes from being stable (when  $a\omega^2 < g$ ) to being unstable (when  $a\omega^2 > g$ ), while  $\theta^* = \pi$  is always present and unstable. Additionally, the stable fixed points  $\theta^* = \pm \arccos(\frac{g}{a\omega^2})$  appear when  $a\omega^2 > g$ . This corresponds to a supercritical pitchfork bifurcation. The system's bifurcation diagram is shown in Fig. 7.23.

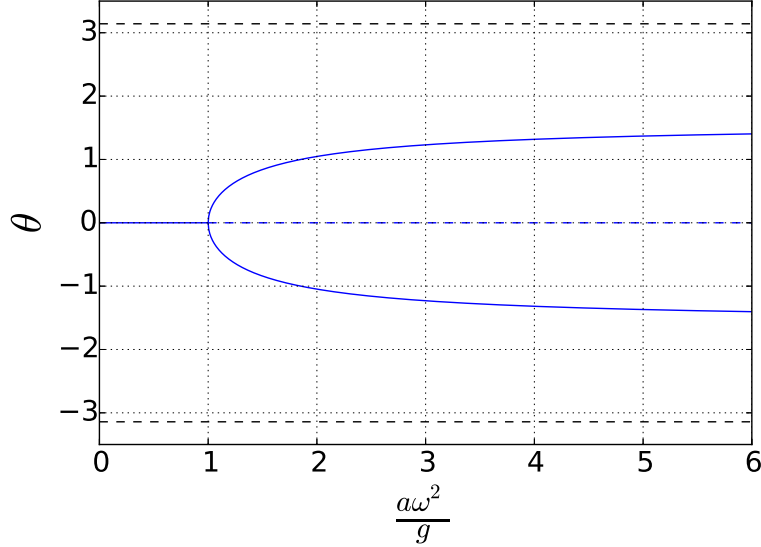


Figure 7.23: When  $\omega^2 > g/a$  the bottom of the loop becomes an unstable fixed point and two new stable fixed points arise that move away from the bottom as the rotation speed is increased.

**Example:** As another example, consider an overdamped pendulum driven by a constant torque described by:

$$\dot{\theta} = \tau - b \sin(\theta), \quad (7.36)$$

where  $\tau > 0$ ,  $b > 0$ , and  $\theta \in [-\pi, \pi]$ . For  $b > \tau$ , the gravity beats the torque and there is one stable and one unstable fixed points as shown in Fig. 7.24. For  $b < \tau$ , there are no fixed points as shown in Fig. 7.25, and here the torque wins resulting in a rotating solution. Even when  $b < \tau$ , there is a remnant of the influence of the fixed point in the slowing down of the pendulum as it goes through the “bottleneck” to overcome gravity. Combined this is thus a saddle-node bifurcation at  $\tau = b$  as shown in Fig. 7.26.

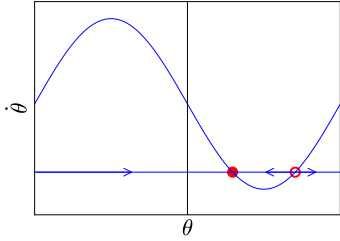


Figure 7.24:  $\dot{\theta}$  as a function of  $\theta$  when  $\tau < b$ . Gravity dominates torque and there is a stable fixed point.

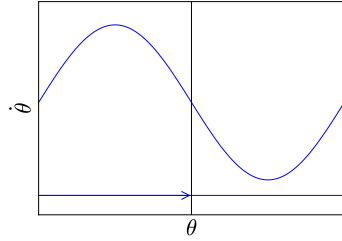


Figure 7.25:  $\dot{\theta}$  as a function of  $\theta$  when  $\tau > b$ . Torque dominates gravity so there are no fixed points.

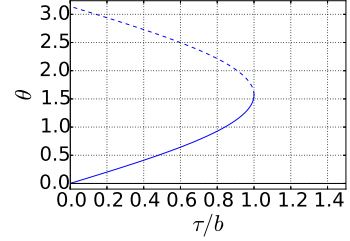


Figure 7.26: Bifurcation plot of the system as a function of the applied torque ( $\tau/b$ ).

## 7.3 Fixed Points in Two-Dimensional Systems

### 7.3.1 Motion Near a Fixed Point

#### General Categorization

In 2-dimensions, to analyze the trajectories near a fixed point  $\vec{x}^* = (x^*, y^*)$ , we can again linearize the equations of the system. Therefore, we'll start by analyzing a general 2-dimensional *linear* system with  $\vec{x}^* = 0$ . This can be written as

$$\begin{aligned}\dot{x} &= ax + by, \\ \dot{y} &= cx + dy,\end{aligned}\tag{7.37}$$

or

$$\dot{\vec{x}} = M\vec{x} \quad \text{where} \quad M = \begin{bmatrix} a & b \\ c & d \end{bmatrix}\tag{7.38}$$

and the matrix of coefficients here has no restrictions.

**Example:** Let us consider a system of equations that consists of two independent 1-dimensional flows,

$$\dot{x} = ax, \quad \dot{y} = -y.\tag{7.39}$$

We have the two independent solutions:

$$x(t) = x_0 e^{at} \quad \text{and} \quad y(t) = y_0 e^{-t}\tag{7.40}$$

The parameter regions  $a < -1$ ,  $a = -1$ , and  $-1 < a < 0$  all produce a stable and attracting fixed point  $\vec{x}^* = 0$  in qualitatively different ways, because the decay rate of  $x(t)$  is

either larger, equal, or smaller than that of  $y(t)$ . This is shown in Figs. 7.27, 7.28, and 7.29. If  $a = 0$ , then  $\vec{x}^* = 0$  is no longer isolated as there is a line of fixed points at  $y = 0$  and for all values of  $x$ , see Fig. 7.30. If  $a > 0$ , then  $\vec{x}^* = 0$  is a saddle point (with the  $y$ -axis being the “stable manifold” and the  $x$ -axis being the “unstable manifold”), see Fig. 7.31.

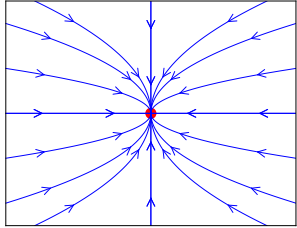


Figure 7.27: Stable Node  
 $a < -1$

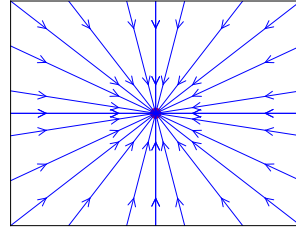


Figure 7.28: Stable Node  
 $a = -1$

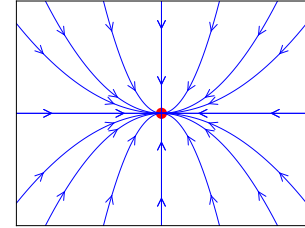


Figure 7.29: Stable Node  
 $-1 < a < 0$

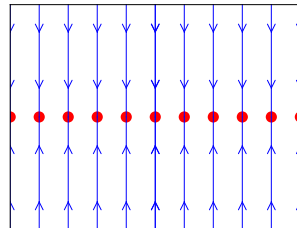


Figure 7.30: Non-isolated fixed points  $a = 0$

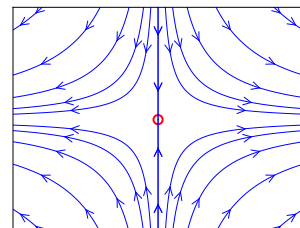


Figure 7.31: Saddle Point  
 $a > 0$

In general in two dimensions there are more possibilities for the motion than in one-dimension and we should be more careful about our definition for when a fixed point is stable. For a fixed point  $\vec{x}^*$  we will say that

- it is *attracting* if all trajectories starting in its neighborhood approach it as  $t \rightarrow \infty$ ,
- it is *Lyapunov stable* if all trajectories starting in its neighborhood remain in that neighborhood for all time,
- it is *stable* if it is both attracting and Lyapunov stable.

Picking one fixed point from Fig. 7.30, most trajectories will be Lyapunov stable but not attracting. If a fixed point allows a trajectory to wander away but eventually return, then it may also be attracting but not Lyapunov stable.

In the general case defined in Eq.(7.38), we need to solve the eigenvalue problem for the linear system, and thus find the eigenvalues and eigenvectors of  $M$ . Here we have

$$\dot{\vec{a}} = M\vec{a} = \lambda\vec{a} \quad \Rightarrow \quad \vec{a}(t) = \vec{a}_0 e^{\lambda t} \quad (7.41)$$

Therefore, as usual, we set  $\det(M - \lambda \mathbb{1}) = 0$  where  $\mathbb{1}$  is the identity matrix of the same dimension as  $M$ . From this, defining

$$\Delta \equiv \det(M) = ac - bd, \quad \tau \equiv \text{tr}(M) = a + d, \quad (7.42)$$

then the eigenvalues are given by

$$\lambda_{\pm} = \frac{\tau \pm \sqrt{\tau^2 - 4\Delta}}{2}. \quad (7.43)$$

The corresponding eigenvectors are then  $\vec{a}_{\pm}$ , and for a generic  $M$  they will not be orthogonal. Assuming that two different eigenvectors exist a general solution is by linearity given by

$$\vec{x}(t) = \text{Re} \left[ C_+ \vec{a}_+ e^{\lambda_+ t} + C_- \vec{a}_- e^{\lambda_- t} \right] \quad (7.44)$$

assuming for the moment that  $\lambda_+ \neq \lambda_-$  and taking the real part at the end if needed. There are three main cases to consider.

1. Real eigenvalues  $\lambda_+, \lambda_- \in \mathbb{R}$  with  $\lambda_+ \neq \lambda_-$ . This is like the system in Eq.(7.40), but with the  $x$  and  $y$  axes replaced by the directions defined by  $\vec{a}_+$  and  $\vec{a}_-$ .

**Example:** Consider for example a solution where  $\vec{a}_+ = (1, 1)$  and  $\vec{a}_- = (1, -4)$ , ignoring normalization. If  $\lambda_- < 0 < \lambda_+$ , then growth occurs along  $\vec{a}_+$  and decay occurs along  $\vec{a}_-$ , so  $\vec{x}^* = 0$  is a saddle point, as drawn in Fig. 7.32

If instead  $\lambda_- < \lambda_+ < 0$ , then decay occurs slower with  $\lambda_+$  so it occurs first onto  $\vec{a}_+$ , making  $\vec{x}^* = 0$  a stable node, as drawn in Fig. 7.33

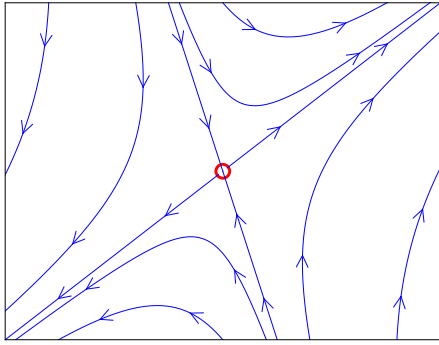


Figure 7.32: Saddle Point with  $\vec{a}_+ = (1, 1)$  and  $\vec{a}_- = (1, -4)$

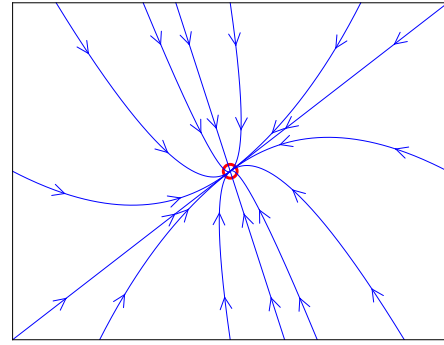


Figure 7.33: Stable Node with  $\vec{a}_+ = (1, 1)$  and  $\vec{a}_- = (1, -4)$

- Let us now consider when  $\lambda_+ = \lambda_- = \lambda \in \mathbb{R}$ . In this situation there can either be two independent eigenvectors or only one. Two independent eigenvectors can only occur if

$$M = \lambda \mathbb{1}, \quad (7.45)$$

in which case the fixed point is called a *star*, and is shown in Fig. 7.34.

If instead there is only one independent eigenvector, then the fixed point is called a *degenerate node*. An example of this is

$$M = \begin{bmatrix} \lambda & b \\ 0 & \lambda \end{bmatrix},$$

where the eigenvalue is  $\lambda$  and which has  $\vec{a} = (1, 0)$  as its only independent eigenvector. Here the phase space portrait is as given in Fig. 7.35, where the trajectory decays first onto the eigenvalue direction and then down onto the fixed point.

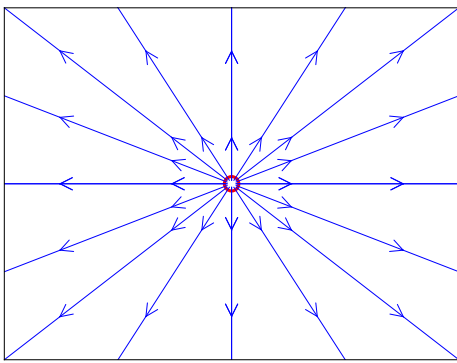


Figure 7.34: Unstable star with  $\lambda > 0$ .

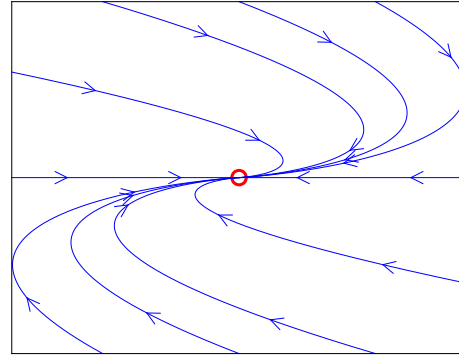


Figure 7.35: Degenerate Node with  $\lambda = -1$  and  $b = 2$ .

3. The final case to consider is when the eigenvalues have complex parts,  $\lambda_{\pm} = \alpha \pm i\omega$  for  $\omega \neq 0$ . If  $\alpha < 0$ , the fixed point is a *stable spiral* where the trajectories spiral into it, as in Fig. 7.36. If  $\alpha = 0$ , the fixed point is a *center*, with neighboring trajectories being closed orbits around it, as in Fig. 7.37. If  $\alpha > 0$ , the fixed point is an *unstable spiral* where trajectories spiral out from it, as in Fig. 7.38.

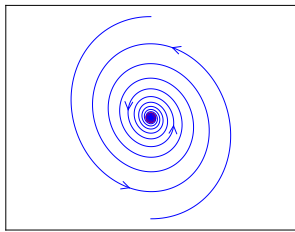


Figure 7.36: Stable spiral with  $\alpha > 0$

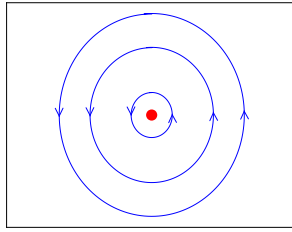


Figure 7.37: Trajectories about a center fixed point

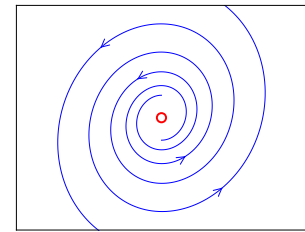


Figure 7.38: Unstable Spiral with  $\alpha < 0$

As a summary if  $\Delta < 0$  then the fixed points are saddle points, while if  $\Delta = 0$  then the fixed points are not isolated but form a continuous line of fixed points. If  $\Delta > 0$ , then there are a number of possibilities:

- $\tau < -2\sqrt{\Delta}$  produces stable nodes;
- $\tau > 2\sqrt{\Delta}$  produces unstable nodes;

- $-2\sqrt{\Delta} < \tau < 0$  produces stable spirals;
- $\tau = 0$  produces centers;
- $0 < \tau < 2\sqrt{\Delta}$  produces unstable spirals;
- $\tau = \pm 2\sqrt{\Delta}$  produces stars or degenerate nodes.

Note that all unstable fixed points have  $\tau > 0$ , while all stable fixed points have  $\tau < 0$ ; this is true even for stars and degenerate nodes. This information can be summarized by the following diagram:

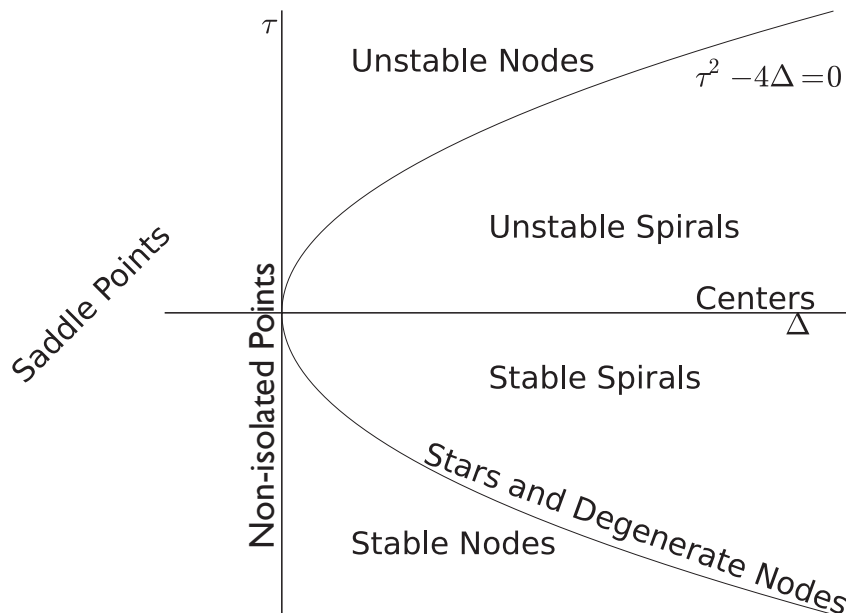


Figure 7.39: Diagram determining the type of fixed point given the determinant  $\Delta$  and trace  $\tau$  of the linearized system.

This linearized analysis yields the correct classification for saddle points, stable/unstable nodes, and stable/unstable spirals, but not necessarily for the borderline cases that occur on a line rather than in an area of the  $\Delta-\tau$  plane (centers, stars, degenerate nodes, or non-isolated fixed points). Nonlinear terms can tip a borderline case to a nearby case in the  $\Delta-\tau$  plane. This implies nonlinear terms may only affect the stability of centers.

#### Analysis of a General 2-Dimensional System

Consider a general 2-dimensional system:

$$\dot{\vec{x}} = \vec{f}(\vec{x}) = (f_x(x, y), f_y(x, y)), \quad (7.46)$$

which may have several fixed points  $(x^*, y^*)$ . We can analyze their types by linearizing about each one, defining  $u = x - x^*$  and  $v = y - y^*$  and expanding about  $(u, v) = (0, 0)$ . Defining  $\vec{u} = (u, v)$ , then this expansion yields

$$\dot{\vec{u}} = M\vec{u} \quad \text{where} \quad M_{ij} = \frac{\partial f_i}{\partial x_j} \Big|_{\vec{x}=\vec{x}^*} \quad (7.47)$$

This is the same as a Taylor series about  $\vec{x} = \vec{x}^*$ , where  $\vec{f}'(\vec{x}^*) = 0$ .

**Example:** Lets consider a population growth model where rabbits ( $x$ ) compete with sheep ( $y$ ). With one species, the model might look like  $\dot{x} = x(1 - x)$ , where for small  $x$  there is population growth, but above  $x > 1$  food resources become scarce and the population shrinks. For two species there can be coupling between the equations, so we could consider

$$\begin{aligned} \dot{x} &= x(3 - x - 2y), \\ \dot{y} &= y(2 - y - x). \end{aligned} \quad (7.48)$$

which is called the Lotka-Volterra model. Here the parameters have been chosen to model the fact that rabbits produce faster ( $3 > 2$  in the linear terms) and sheep compete better for resources ( $2 > 1$  in the quadratic cross terms). To determine how solutions to these equations behave we can analyze the structure of the fixed points.

The fixed points for this system are:

$$\vec{x} \in \{(0, 0), (0, 2), (3, 0), (1, 1)\} \quad (7.49)$$

For each one we carry out a linear analysis:

- $\vec{x}^* = (0, 0)$  simply gives  $\dot{x} = 3x$  and  $\dot{y} = 2y$ , so it is an unstable node.
- $\vec{x}^* = (0, 2)$ . Here we define  $u = x$  and  $v = y - 2$  and the linear equations become  $\dot{u} = -u$  and  $\dot{v} = -2u - 2v$ . Taking the trace and determinant we find  $\tau = -3$  and  $\Delta = 2$  giving  $\lambda_+ = -1$  and  $\lambda_- = -2$ . This is a stable node.
- $\vec{x}^* = (2, 0)$  gives  $\lambda_+ = -1$  and  $\lambda_- = -3$ , making it too a stable node.
- $\vec{x}^* = (1, 1)$  gives  $\lambda_\pm = -1 \pm \sqrt{2}$ , making it a saddle point.

From knowing the behavior of trajectories near these fixed points we can complete the picture for an approximate behavior of the entire system, as shown in Fig. 7.40. A diagonal line passing through the unstable node and saddle point divides the basins of attraction for the fixed points where the sheep win  $(0, 2)$  or where the rabbits win  $(3, 0)$ .

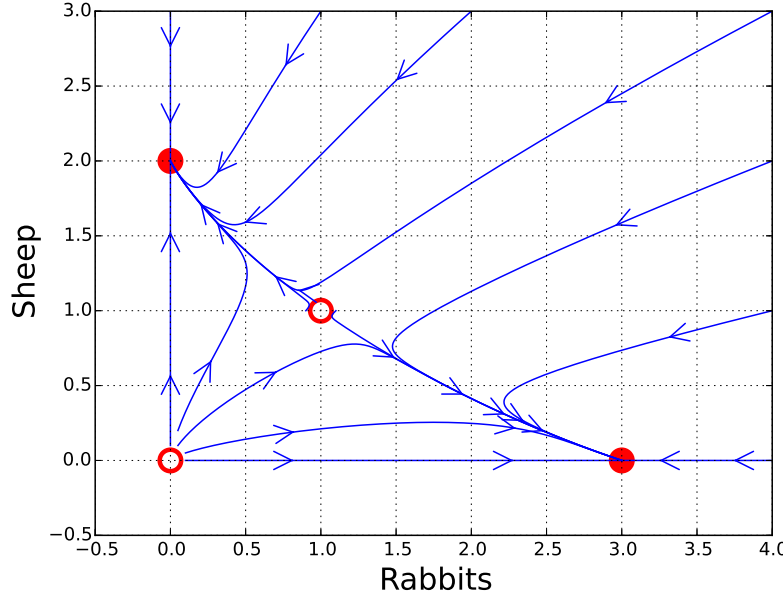


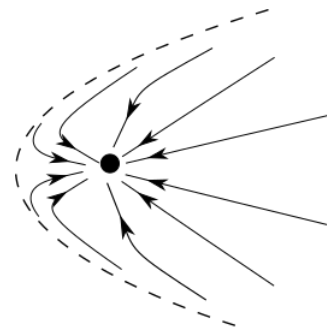
Figure 7.40: Picture of the behavior of trajectories for the population growth model in Eq. (7.48).

### 7.3.2 Systems with a conserved $E(\vec{x})$

The mechanical systems of equations that we are most familiar with are those where the energy is constant along trajectories. We will generalize this slightly and say systems with *any* function  $E = E(\vec{x})$  that is conserved (so  $\dot{E} = 0$ ) are *conservative systems with  $E$* . To rule out taking a trivial constant value of  $E$  (which would work for any system), we demand that  $E(\vec{x})$  must not be constant on any closed region in the space of  $\vec{x}$ . Note that  $\dot{E} = 0$  is generally not equivalent to  $\nabla \cdot \vec{f} = 0$ , and hence we do not simply call these conservative systems.

Several results follow from considering conservative systems with an  $E$ :

- Conservative systems with  $E$  do not have attracting fixed points. We can prove this by contradiction, by imagining that such a point did exist. Since all the points in the basin of attraction of that point must go to this single fixed point, they must all share the same value of  $E$ , which contradicts  $E$  not being constant within a closed region.



- From our experience in expanding about the minima of potentials, we also expect to find stable centers for conservative systems with  $E$ . This result is achieved by the following theorem which we have essentially proven in our analysis in the chapter on vibrations:

For  $\dot{\vec{x}} = \vec{f}(\vec{x})$ , where  $\frac{\partial f_i}{\partial x_j}$  is continuous for all  $i, j$ , if  $E = E(\vec{x})$  is conserved with an isolated fixed point  $\vec{x}^*$  at the minimum of  $E$ , then all trajectories sufficiently close are centers.

- In 2 dimensions the  $\nabla \cdot \vec{f} = 0$  definition of conservative is equivalent to having a conserved  $E = E(\vec{x})$  along the systems trajectories.

Knowing that  $\dot{\vec{x}} = \vec{f}(\vec{x})$  and  $\nabla \cdot \vec{f} = 0$ , then let us define:

$$\begin{aligned} H(\vec{x}) &= \int^y f_x(x, y') dy' - \int^x f_y(x', y) dx' \\ &\Rightarrow \frac{\partial H}{\partial y} = f_x(x, y) - \int^x \frac{\partial f_y(x', y)}{\partial y} dx' = f_x + \int^x \frac{\partial f_x(x', y)}{\partial x'} dx' \\ &\Rightarrow \frac{\partial H}{\partial x} = -f_y(x, y) + \int^y \frac{\partial f_x(x, y')}{\partial x} dy' = -f_y - \int^y \frac{\partial f_y(x, y')}{\partial y'} dy' \end{aligned} \quad (7.50)$$

Then  $\frac{\partial H}{\partial y} \in \{f_x, 2f_x\}$  and  $\frac{\partial H}{\partial x} \in \{-f_y, -2f_y\}$ . The first case of each occurs if  $f_x = f_x(y)$  and  $f_y = f_y(x)$ , respectively. Thus  $\dot{x} = \mu \frac{\partial H}{\partial y}$  and  $\dot{y} = -\mu \frac{\partial H}{\partial x}$  for  $\mu \in \{1, 2\}$ . After a trivial rescaling, these are the Hamilton equations for a conserved Hamiltonian  $H(\vec{x})$  (independent of  $t$ ) which serves here as our function  $E(\vec{x})$ . Additionally, from the relations the critical points  $\vec{x}^*$  of  $H$  where  $\nabla H|_{\vec{x}=\vec{x}^*} = 0$  are identical to the fixed points where  $\vec{f}(\vec{x}^*) = 0$ .

**Example:** Consider the one-dimensional classical mechanics motion given by:

$$\ddot{x} = ax - x^2 \equiv -U'(x) \quad (7.51)$$

with  $a > 0$ . We first turn this into one-dimensional form by writing

$$\dot{x} = y = f_x, \quad \dot{y} = ax - x^2 = f_y. \Rightarrow \quad (7.52)$$

Since here  $f_x$  is independent of  $x$ , and  $f_y$  is independent of  $y$ , we obviously have  $\nabla \cdot \vec{f} = 0$ . We can define a conserved scalar quantity from  $f_x$  and  $f_y$  using Eq. (7.50) to give

$$H = \frac{y^2}{2} - \frac{ax^2}{2} + \frac{x^3}{3} = K(y) + U(x) \quad (7.53)$$

where we have Hamilton's equations

$$\dot{x} = \frac{\partial H}{\partial y} = \frac{\partial K}{\partial y} \quad \text{and} \quad \dot{y} = -\frac{\partial H}{\partial x} = -\frac{\partial U}{\partial x}. \quad (7.54)$$

For this system the fixed points occur at  $\vec{x}^* = (0, 0)$  and  $(a, 0)$ , which are also the extremal points of  $H$ . For  $\vec{x}^* = (0, 0)$  we have

$$\frac{\partial^2 H}{\partial a^2} = -a < 0 \quad , \quad \frac{\partial^2 H}{\partial y^2} = 1 > 0 \quad , \quad \text{and} \quad \frac{\partial^2 H}{\partial x \partial y} = 0 , \quad (7.55)$$

so the fixed point is a saddle point. For  $\vec{x}^* = (a, 0)$  we have

$$\frac{\partial^2 H}{\partial x^2} = a > 0 \quad , \quad \frac{\partial^2 H}{\partial y^2} = 1 > 0 \quad , \quad \text{and} \quad \frac{\partial^2 H}{\partial x \partial y} = 0 , \quad (7.56)$$

so the fixed point is a center. These fixed points and some representative trajectories are illustrated in Fig. 7.41. Here the bound trajectories have  $H < 0$ , while the unbound trajectories have  $H > 0$ . The dividing case with energy  $H = 0$  is the trajectory that would stop at the saddle point  $(0, 0)$ .

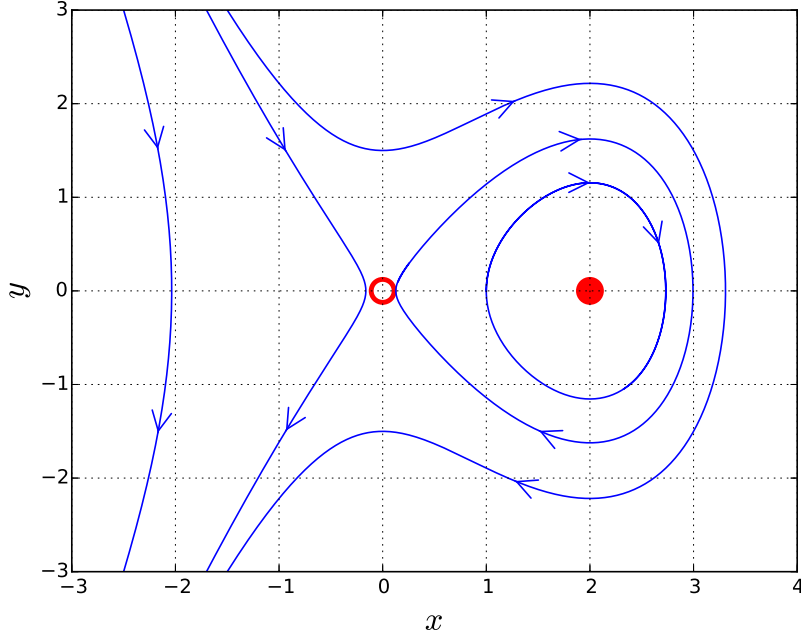


Figure 7.41: Phase space picture of the system  $\ddot{x} = ax - x^2$  with  $a = 2$ .

## 7.4 Limit Cycles and Bifurcations

In two dimensions, we can have a new type of 2-dimensional attractor called a *limit cycle*, which is an isolated closed trajectory. For stable limit cycles nearby converge to it as in Fig. 7.42, while for unstable limit cycles the nearby trajectories diverge from it as in

Fig. 7.43. We could also imagine a semi-stable limit cycles, where the trajectories converge or diverge on opposite sides of the cycle (an example is shown in Fig. 7.44).

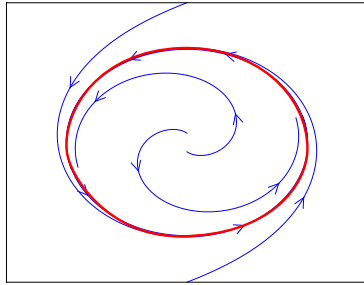


Figure 7.42: Stable Limit Cycle

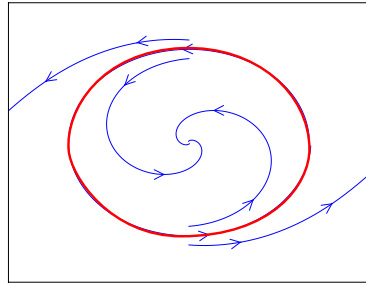


Figure 7.43: Unstable limit Cycle

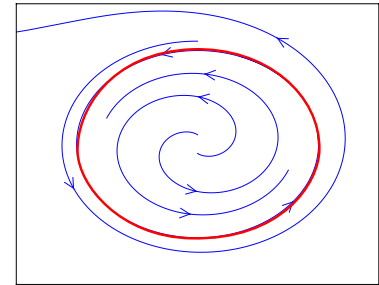


Figure 7.44: Semi-stable Limit Cycle

Note that a limit cycle is not like a center trajectory about a fixed point, because a limit cycle is isolated from other closed trajectories, whereas around centers nearby trajectories are also closed.

**Example:** Lets consider a system of equations written with polar coordinates,  $x = r \cos(\theta)$  and  $y = r \sin(\theta)$  so that

$$\dot{r} = r(1 - r^2), \quad \dot{\theta} = 1, \quad (7.57)$$

with  $r \geq 0$ . Here the circle  $r^* = 1$  corresponds to a stable limit cycle, as in Fig. 7.42. Since only the radial coordinate matters for the stability of the limit cycle we can picture this in one dimension, as in Fig. 7.45.

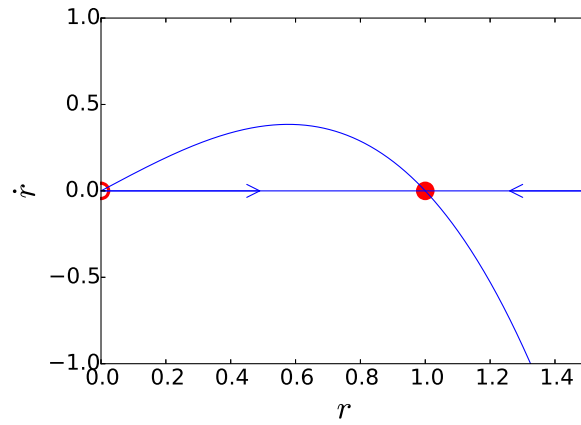


Figure 7.45: Behavior of the radial component of the system. The stable point is at  $r = 1$ , meaning the system has a stable limit cycle of radius  $r = 1$ .

**Example:** Lets consider the van der Pol oscillator (first studied in 1927 in electric circuits and found to exhibit chaotic “noise” when driven)

$$\ddot{x} + \mu(x^2 - 1)\dot{x} + x = 0 \Rightarrow \begin{cases} \dot{x} = \omega \\ \dot{\omega} = \mu(1 - x^2)\omega - x \end{cases} \quad (7.58)$$

If  $x^2 > 1$  then the term involving  $\mu$  gives (nonlinear) positive damping, while if  $x^2 < 1$  then the term involving  $\mu$  gives (nonlinear) negative damping, which is growth. For different  $\mu$  values the phase portrait is depicted in the figures below.

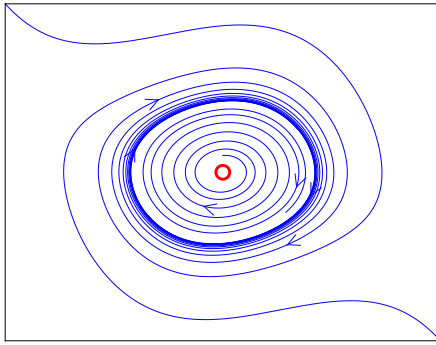


Figure 7.46: Van Der Pol Oscillator with  $\mu = 0.1$

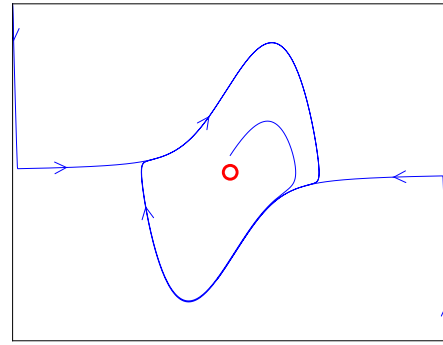


Figure 7.47: Van Der Pol Oscillator with  $\mu = 2$

There are several known methods for ruling out limit cycles, but we will instead focus on a method for showing they exist.

### 7.4.1 Poincaré-Bendixson Theorem

Take a 2-dimensional system  $\dot{x} = f_x(x, y)$  and  $\dot{y} = f_y(x, y)$  with continuous and differentiable  $f$ . Let  $\mathbb{D}$  be a closed, bounded region. Suppose there exists a trajectory  $C$  confined inside  $\mathbb{D}$  for all times  $t \geq 0$ , then  $C$  either goes to a fixed point or a limit cycle as  $t \rightarrow \infty$ .

The proof requires the use of some topology, so we won’t study it. To understand how we can use this theorem, let us suppose we have determined that there are no fixed points in a closed, bounded region  $\mathbb{D}$ , and at the boundary’s surface the  $\dot{x}$  points “inward” to trap the trajectory in  $\mathbb{D}$ . An example of this situation is shown in Fig.(7.48). Then due to the theorem we must have a limit cycle in this region. Intuitively, the trajectory  $C$  wanders around  $\mathbb{D}$ , but it cannot self intersect and it eventually runs out of room to wander. Therefore, it must converge to a fixed point or a limit cycle. This implies that there is *no chaos in 2 dimensions*.

In 3 or more dimensions, trajectories have “more room” to wander and can do so forever, allowing for chaos!

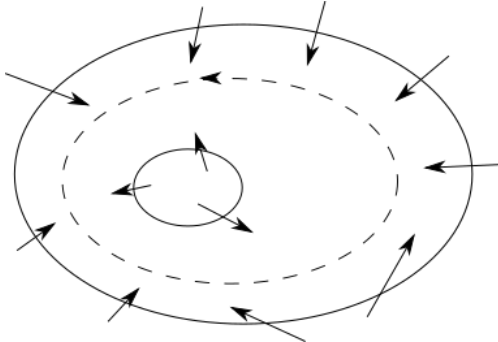


Figure 7.48: If at the boundary, the flow of a two-dimensional system pushes it into a region where there are no fixed points, then the system has a stable limit cycle in that region.

**Example:** Lets consider whether a limit cycle exists for

$$\begin{cases} \dot{x} = x - y - x(x^2 + 5y^2) \\ \dot{y} = x + y - y(x^2 + y^2) \end{cases} \quad (7.59)$$

Using polar coordinates

$$r\dot{r} = x\dot{x} + y\dot{y} \Rightarrow r\dot{r} = r^2(1 - r^2 - r^2 \sin^2(2\theta)) \quad (7.60)$$

In particular,  $1 - r^2 - r^2 \sin^2(2\theta) > 0$  for  $r < 1/\sqrt{2}$ , while  $1 - r^2 - r^2 \sin^2(2\theta) < 0$  for  $r > 1$ . Since there are no fixed points for  $1/\sqrt{2} < r < 1$  there must be a limit cycle.

### 7.4.2 Fixed Point Bifurcations Revisited and Hopf Bifurcations

We can revisit bifurcations by adding a varying parameter to the discussion of fixed points and limit cycles. In particular, we now include limit cycles popping in or out of existence in the range of things that can occur if we change a parameter.

Saddle-node, transcritical, and pitchfork bifurcations for fixed points can still occur here.

**Example:** As a simple example consider a system of uncoupled equations

$$\dot{x} = \mu - x^2, \quad \dot{y} = -y. \quad (7.61)$$

which has a saddle-node bifurcation at  $\mu = 0$ , as shown in the phase portraits below.

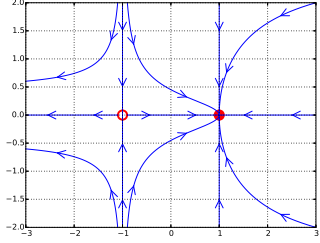


Figure 7.49: System with  $\mu = 1$  with two fixed points

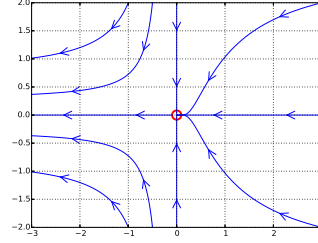


Figure 7.50: System with  $\mu = 0$  and one fixed point

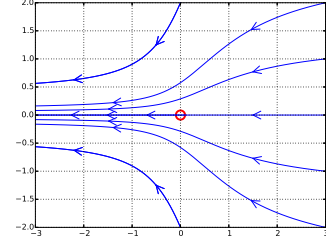


Figure 7.51: System with  $\mu = -1$  and no fixed points

More generally, we can think about determining the fixed points by drawing the curves  $\dot{x} = f_x(x, y) = 0$  and  $\dot{y} = f_y(x, y) = 0$  separately. Fixed points require both equalities to be satisfied, so we look for crossings of these two curves. Varying a parameter of the system then leads the fixed points to slide into one another, which corresponds to a 1-dimensional motion. This is why our study of the various types of bifurcation of fixed points in one-dimension (saddle-node, transcritical, supercritical and subcritical pitchforks) immediately carry over to bifurcation of fixed points in higher dimensional equations.

**Example:** consider the system of equations

$$\dot{x} = \mu x + y + \sin(x), \quad \dot{y} = x - y. \quad (7.62)$$

Note that these equations have a symmetry under  $x \rightarrow -x$  and  $y \rightarrow -y$ . This always has  $\vec{x}^* = (0, 0)$  as a fixed point. Linearizing for this fixed point yields  $\tau = \mu$  and  $\Delta = -(\mu + 2)$ . So the fixed point is stable if  $\mu < -2$  or a saddle point if  $\mu > -2$ .

Due to the symmetry we might expect a pitchfork bifurcation. If so, then near  $\mu = -2$ , there should be two more fixed points. We would need  $x = y$ , so expanding and solving we write

$$\dot{x} = (\mu + 1)x + x - \frac{x^3}{6} + \dots = 0. \quad (7.63)$$

Since we are studying points near  $x \simeq 0$ , but with  $\mu \simeq -2$  the term with  $x^3$  can be equally important, whereas the higher terms are subleading. This yields a solution where  $x^* = y^* = \pm\sqrt{6(\mu + 2)}$  for  $\mu > -2$ , implying that there is a supercritical pitchfork bifurcation. This occurs when  $\Delta = \lambda_+ \lambda_- = 0$ , which actually means  $\lambda_+ = 0$  first. As we vary  $\mu$  here the eigenvalue crosses from negative to positive values and the stability changes.

### Hopf Bifurcations

A *Hopf bifurcation* occurs when a spiral trajectory changes stability when a parameter is varied, and this stability change is accompanied by the creation or destruction of limit

cycles. A Hopf bifurcation is like a pitchfork bifurcation except that the limit cycle replaces the “fork” in the pitchfork. Both supercritical and subcritical Hopf bifurcations exist in analogy to pitchfork bifurcations. Here the transition of the eigenvalues of the linearized system is different, with the real part of both eigenvalues switching sign simultaneously, as pictured below:

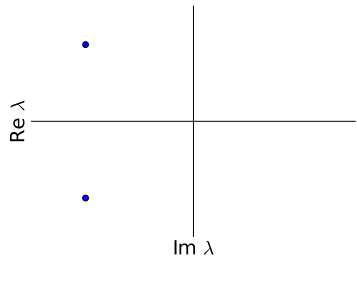


Figure 7.52:  $\text{Re}(\lambda) < 0$   
which gives us a stable spiral

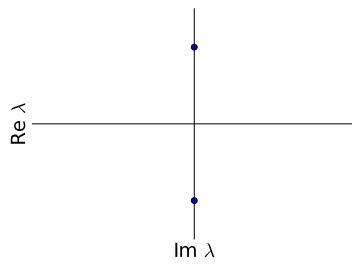


Figure 7.53:  $\text{Re}(\lambda) = 0$

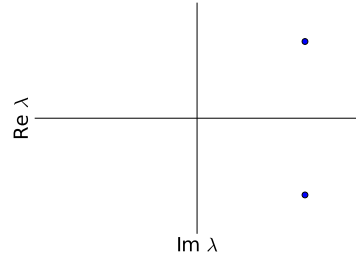


Figure 7.54:  $\text{Re}(\lambda) > 0$   
which gives us an unstable spiral

**Example:** Consider in polar coordinates the system

$$\dot{r} = \mu r - r^3, \quad \dot{\theta} = \omega + br^2. \quad (7.64)$$

It has a stable spiral into  $r^* = 0$  for  $\mu < 0$  and no limit cycles. For  $\mu > 0$ , then  $r^* = \sqrt{\mu}$  is a stable limit cycle, while the spiral from  $r^* = 0$  becomes unstable. Thus,  $\mu = 0$  is a supercritical Hopf bifurcation.

If we look at the eigenvalues of the linearized system at  $r = 0$  by setting  $x = r \cos(\theta)$  and  $y = r \sin(\theta)$ , then  $\dot{x} \approx \mu x - \omega y$  and  $\dot{y} \approx \omega x + \mu y$ , so  $\lambda_{\pm} = \mu \pm i\omega$  which indeed hits  $\text{Re}(\lambda) = 0$  when  $\mu = 0$  as expected. The flows for this Hopf bifurcation are depicted below.

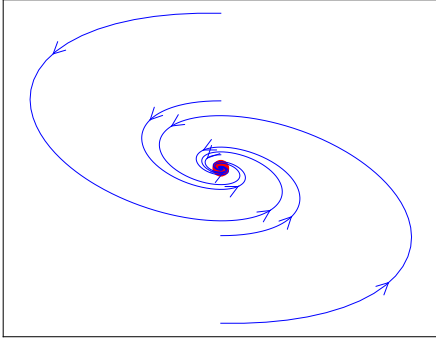


Figure 7.55: System for  $\mu = -0.5$ ,  $b = 2$  and  $\omega = 1$

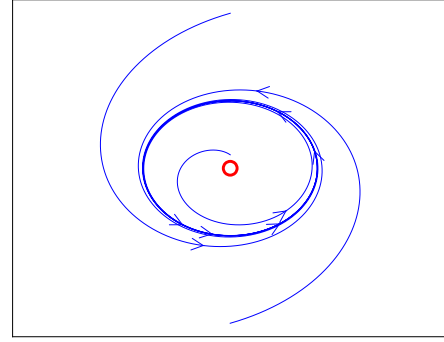


Figure 7.56: System for  $\mu = 1$ ,  $b = 2$  and  $\omega = 1$

**Example:** Consider the following system of equations in polar coordinates:

$$\dot{r} = \mu r + r^3 - r^5, \quad \dot{\theta} = \omega + br^2, \quad (7.65)$$

which has a subcritical Hopf bifurcation at  $\mu = 0$ .

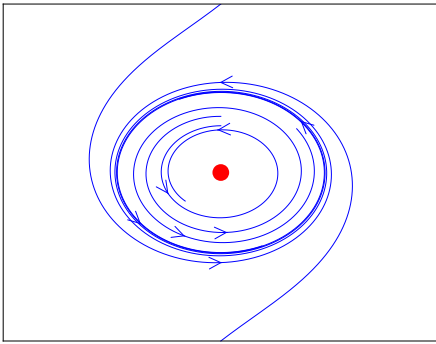


Figure 7.57: System for  $\mu = -0.2$ ,  $b = 2$  and  $\omega = 1$ . One of the inner orbits converges to the center while the other converges to the outer limit cycle, there is an unstable limit cycle between the two.

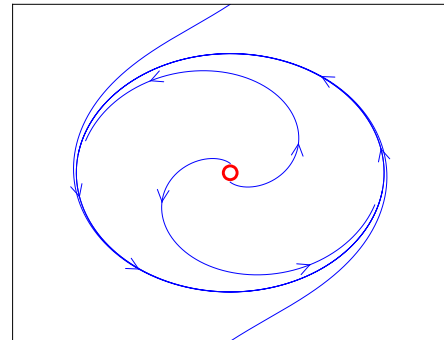


Figure 7.58: System for  $\mu = 1$ ,  $b = 2$  and  $\omega = 1$ . There is no longer an unstable limit cycle in the inner region of the phase space.

**Example:** As a physics example with a limit cycle, let's consider a damped pendulum driven

by a constant torque whose equation of motion is

$$\ddot{\theta} + \frac{1}{q}\dot{\theta} + \sin(\theta) = \tau \quad \Rightarrow \quad \begin{cases} \dot{\theta} = \omega \\ \dot{\omega} = -\frac{1}{q}\omega - \sin(\theta) + \tau \end{cases} \quad (7.66)$$

For  $\tau \leq 1$ , the fixed points are  $\omega^* = 0$  and  $\sin(\theta^*) = \tau$ , for which there are two solutions given by the solutions to  $\theta^* = \arcsin(\tau)$ . The graphical solution for the fixed points is shown below where we compare  $\sin \theta$  to the constant  $\tau$  and observe where they cross. One fixed point is stable and the other is a saddle point.<sup>2</sup>

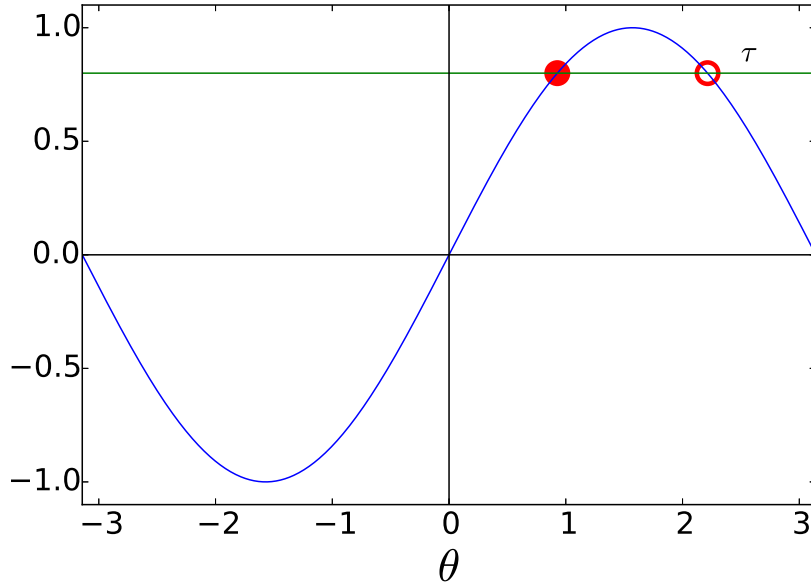


Figure 7.59: Graphical determination of the  $\theta$  value of the fixed points. We see that they cannot occur if  $\tau > 1$ .

What if  $\tau > 1$ ? It turns out that there is a unique stable limit cycle attractor. Consider

$$\dot{\omega} = -\frac{1}{q}[\omega - q(\tau - \sin \theta)] \quad (7.67)$$

For  $\tau > 1$  there are no fixed points, however for very negative  $\omega$ , then  $\dot{\omega} > 0$  and for very positive  $\omega$ ,  $\dot{\omega} < 0$ . There is thus a trapping region where the system has no fixed points, which by the Poincaré-Bendixson theorem implies the existence of a limit cycle. This limit

<sup>2</sup>See also our earlier analysis of the overdamped oscillator in Eq. (7.35), which used a slightly different definition for the constants ( $q\tau \rightarrow \tau$  and  $q \rightarrow b$ ).

cycle corresponding to rotations of the pendulum over the top. The motion of two trajectories with the same initial conditions, but with  $\tau < 1$  and  $\tau > 1$ , are shown in Fig. 7.60.

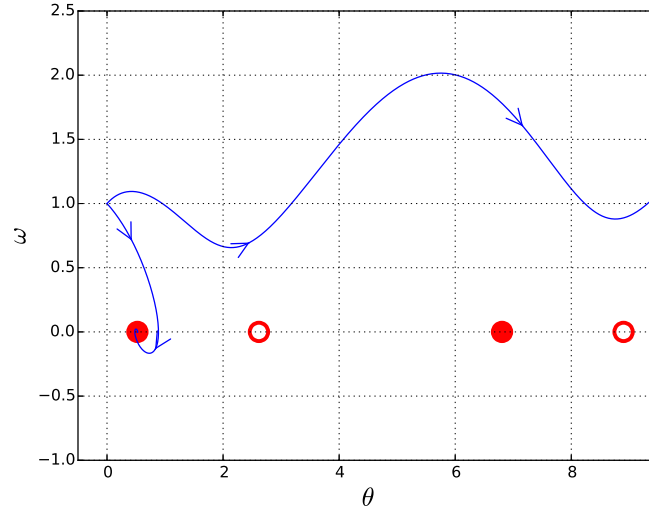


Figure 7.60: Two trajectories shown from the same initial condition, one with  $\tau < 1$  (where the trajectory converges to stable point), and one with  $\tau > 1$  (where the trajectory continues indefinitely).

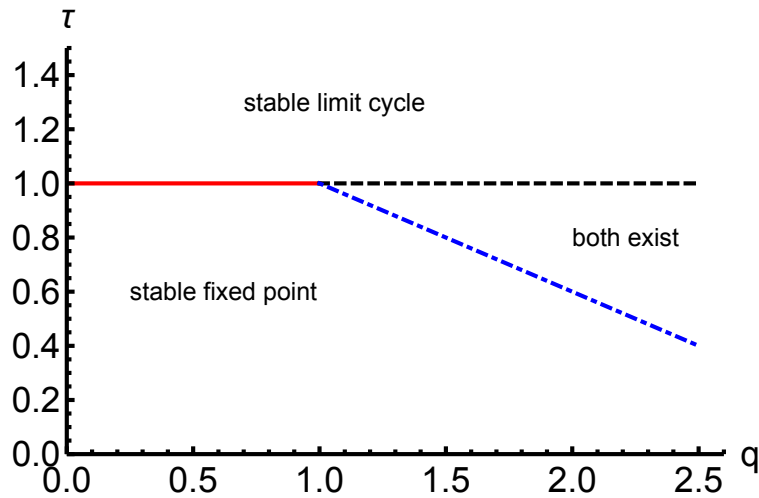


Figure 7.61: Stable attractors and bifurcation transitions for a pendulum with a constant applied torque.

In fact for  $q > 1$  the limit cycle also exists for a range of values  $\tau_c < \tau < 1$ . Since both the fixed points and limit cycle exist for these parameter values the endpoint of the motion

depends on the choice of initial conditions. Here  $\tau_c$  is a constant that depends on  $q$ , and as  $q \rightarrow 1$  then  $\tau_c \rightarrow 1$ . For  $q \leq 1$  the limit cycle only exists for  $\tau \geq 1$ . The boundaries between these regions are sketched in Fig. 7.61. For the transition between the cycle and fixed points shown as a solid (red) line, the saddle and stable node fixed points are born on the cycle which then disappears (called an  $\infty$ -period bifurcation). The transition across the dashed (black) line is a saddle node bifurcation where the two fixed points are born, but the saddle persists. Finally, for the transition across the dot-dashed (blue) line the saddle point collides with and destabilizes the cycle, so that it seeks to exist in the region to the left (this is called a homoclinic bifurcation). Although we have not tried to classify the full range of possible bifurcations for systems involving a limit cycle, this example has illustrated a few of the possibilities.

## 7.5 Chaos in Maps

In nonlinear systems with 2 variables, we have obtained a qualitative analytic understanding of the motion by analyzing fixed points and limit cycles. The analysis of 2 variables includes the possible motion for a 1-dimensional particle with two phase space variables. There is no chaos with 2 variables. We could study chaos with 3 variables, but is there a simpler way?

Recall that chaos in the Poincaré map of the damped driven nonlinear oscillator could be found from

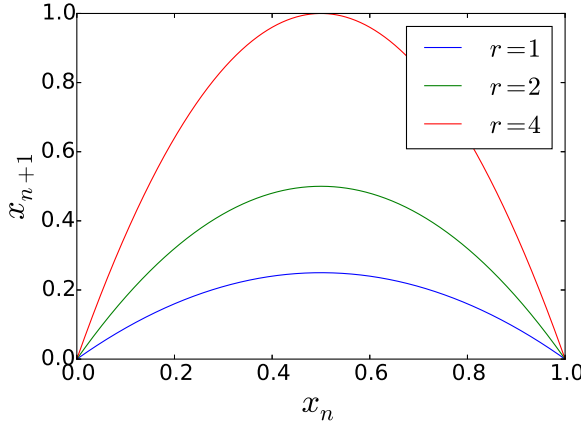
$$\begin{cases} \theta_{N+1} = f_1(\theta_N, \omega_N) \\ \omega_{N+1} = f_2(\theta_N, \omega_N) \end{cases} \quad (7.68)$$

which are 2 discrete variables. Here we set  $\varphi = 2\pi N$  to be discrete with  $N$  an integer. Uniqueness for the 3 continuous variable solution implies the existence of  $f_1$  and  $f_2$ . In fact, for general systems, we can go a step further. Chaos already exists in 1-dimensional maps  $x_{N+1} = f(x_N)$  for a nonlinear function  $f$ .

The example we will be using to illustrate chaos in maps is the logistic map:

$$x_{n+1} = f(x_n) = rx_n(1 - x_n) \quad (7.69)$$

which has a parameter  $r$ . If we take  $0 < r \leq 4$ , then the  $\{x_n\}$  are bounded by  $0 \leq x \leq 1$ , since the maximum is  $f(1/2) = r/4$ . We can visualize this solution by a plot in the  $x_n$ - $x_{n+1}$  plane:



The fixed points of a general map satisfy:

$$x^* = f(x^*) \quad (7.70)$$

which is slightly different from nonlinear differential equations, as these are now iterated difference equations. For our logistic map example this gives

$$x^* = rx^*(1 - x^*) \Rightarrow \begin{cases} x^* = 0 & \text{for all } r \\ x^* = 1 - \frac{1}{r} & \text{for } r > 1 \end{cases} \quad (7.71)$$

The stability of a fixed point can be found by checking a small perturbation

$$x_N = x^* + \eta_N \Rightarrow x_{N+1} = x^* + \eta_{N+1} = f(x^* + \eta_N) = f(x^*) + \left. \frac{df}{dx} \right|_{x=x^*} \eta_N + O(\eta^2) \quad (7.72)$$

to obtain

$$\eta_{N+1} = \left. \frac{df}{dx} \right|_{x=x^*} \eta_N \quad (7.73)$$

Therefore if

- $\left| \frac{df}{dx} \right|_{x=x^*} < 1 \Rightarrow \lim_{N \rightarrow \infty} \eta_N = 0$ :  $x^*$  is stable.
- $\left| \frac{df}{dx} \right|_{x=x^*} > 1 \Rightarrow \lim_{N \rightarrow \infty} \eta_N \rightarrow \infty$ :  $x^*$  is unstable.
- $\left| \frac{df}{dx} \right|_{x=x^*} = 1$ , then  $x^*$  is marginal (requiring an expansion beyond linear analysis).

For the logistic map, Eq. (7.69) we have:

$$\frac{df}{dx} = r - 2rx \Rightarrow \begin{cases} \left. \frac{df}{dx} \right|_{x=0} = r & x^* = 0 \\ \left. \frac{df}{dx} \right|_{x=x^*} = 2 - r & x^* = 1 - \frac{1}{r} \end{cases} \quad (7.74)$$

The first case is stable if  $r < 1$ , and the second is stable if  $1 < r < 3$  and unstable otherwise, which we show graphically in Fig. 7.62. Thus we find that

$$\lim_{n \rightarrow \infty} x_n = \begin{cases} 0 & r < 1 \\ 1 - \frac{1}{r} & 1 < r < 3 \end{cases} . \quad (7.75)$$

For  $r > 3$ , the  $\lim_{N \rightarrow \infty} x_N$  is not well-defined as a single number given by a fixed point. So what happens?

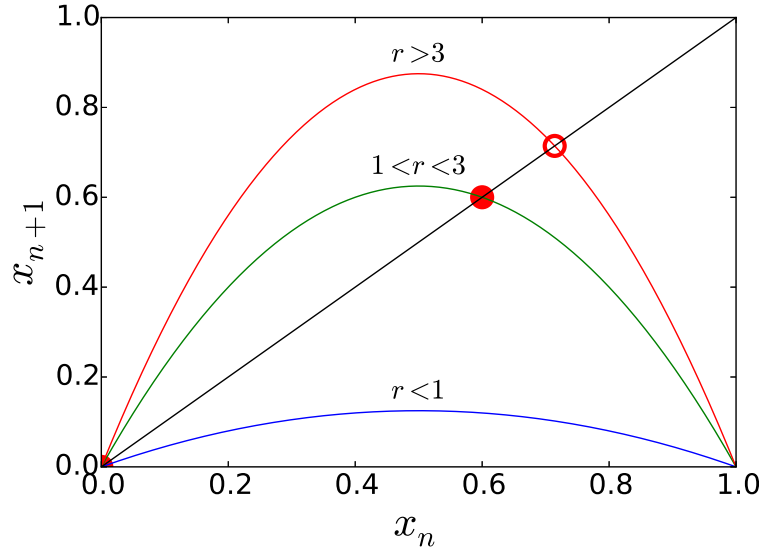


Figure 7.62: Stability of fixed points of the Logistic Map.

To find out, consider two iterations of the map:

$$x_{n+2} = f(f(x_n)) \quad (7.76)$$

which makes  $x_{n+2}$  a 4<sup>th</sup> order polynomial of  $x_n$  as shown in Fig. 7.63 on the right. Here there are three fixed points of the double iterated map, two are stable (which we call  $p$  and  $q$ ) and one is unstable. Furthermore we find that  $p = f(q)$  and  $q = f(p)$ , so the  $n \rightarrow \infty$  state of the

Logistic map is an oscillating 2-cycle as shown in Fig. 7.63 on the left. Thus the (discrete) period has doubled and we call this a pitchfork bifurcation of the map at  $r = 3$ .

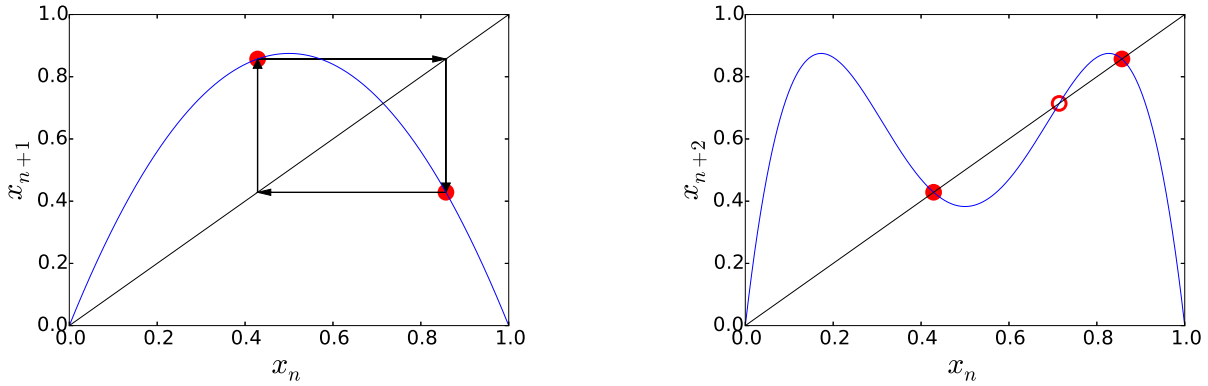


Figure 7.63: The logistic map for  $r > 3$  has fixed points for the double iterated mapping, which are a two-cycle for the original map.

If we analyze the stability of  $p$  and  $q$ , we find that more bifurcations occur for higher values of  $r$ . Since

$$\frac{d}{dx} (f(f(x)))|_{x=x^*} = \frac{df(p)}{dp} \frac{df(q)}{dq} \quad (7.77)$$

for  $x^* = p$  or  $x^* = q$ , this implies that  $p$  and  $q$  lose their stability simultaneously when  $\left| \frac{df(p)}{dp} \frac{df(q)}{dq} \right| > 1$ . At this point the 2-cycle bifurcates into a 4-cycle. This pattern of period doubling continues,  $2 \rightarrow 4 \rightarrow 8 \rightarrow 16 \rightarrow 32 \rightarrow \dots$ , until  $r = 3.5699456\dots$ . Beyond that point the map becomes chaotic. This behavior is shown in Fig. 7.64.

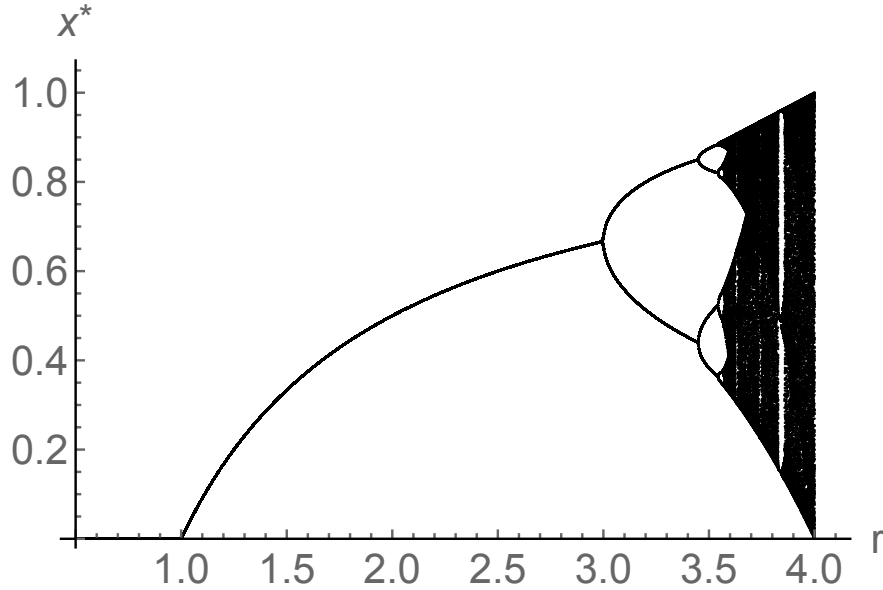


Figure 7.64: Bifurcation plot for the Logistic Map, showing points that are part of the non-transient motion as a function of  $r$ . Below  $r = 3$  there is a single fixed point. The first two bifurcations occur for  $r = 3$  and  $r = 1 + \sqrt{6}$ . Each new bifurcation is closer to the previous, until we reach the chaotic regime. In the middle of the chaotic region there are non-chaotic regions, such as the one near  $r = 0.384$  visible as a white stripe.

This is called a *period doubling road to chaos* and is one common mechanism by which chaos emerges. Indeed, this phenomena also occurs in the nonlinear damped driven oscillator. But how do we know that it is chaos?

If chaos occurs in a map, then we should have sensitivity to initial conditions. Examine

$$\begin{aligned} x_0 &\rightarrow x_1 \rightarrow x_2 \rightarrow \dots \\ x_0 + \delta_0 &\rightarrow x_1 + \delta_1 \rightarrow x_2 + \delta_2 \rightarrow \dots \end{aligned}$$

where  $\delta_n$  is the separation between two initially neighboring trajectories after  $n$  iterations. As such we expect  $\lim_{n \gg 1} |\delta_n| \approx |\delta_0| e^{\lambda n}$ ; there should be exponential separation with  $\lambda > 0$  for chaos to occur, where  $\lambda$  is called the *Lyapunov exponent*.

For maps we can derive a formula for  $\lambda$  as follows. We know that:

$$\lambda = \lim_{n \rightarrow \infty} \frac{1}{n} \ln \left| \frac{\delta_n}{\delta_0} \right| = \lim_{n \rightarrow \infty} \frac{1}{n} \ln \left| \frac{f^n(x_0 + \delta_0) - f^n(x_0)}{\delta_0} \right| \quad (7.78)$$

where  $f^n(x) = \underbrace{f(f(f(\dots x)))}_{n \text{ times}}$ . Assuming that  $\delta_0$  is very small this implies

$$\lambda \simeq \lim_{n \rightarrow \infty} \frac{1}{n} \ln \left| \frac{d}{dx_0} f^n(x_0) \right| = \lim_{n \rightarrow \infty} \frac{1}{n} \ln \left| \prod_{j=0}^{n-1} \frac{df(x_j)}{dx_j} \right|, \quad (7.79)$$

where the  $x_j$  are the points along the map trajectory so far. This gives

$$\lambda = \lim_{n \rightarrow \infty} \frac{1}{n} \sum_{j=0}^{n-1} \ln \left| \frac{df(x_j)}{dx_j} \right| \quad (7.80)$$

as a formula we can use to compute the Lyapunov exponent by keeping track of this sum as we increase  $n$ . The result is shown in Fig. 7.65. In period doubling regions  $\lambda < 0$ , while in chaotic regions  $\lambda > 0$ . There may also be periodic windows with chaos on either side. For the logistic map, the largest such window is the 3-cycle near  $r \approx 3.83$ . These windows are also clearly visible in the bifurcation diagram.

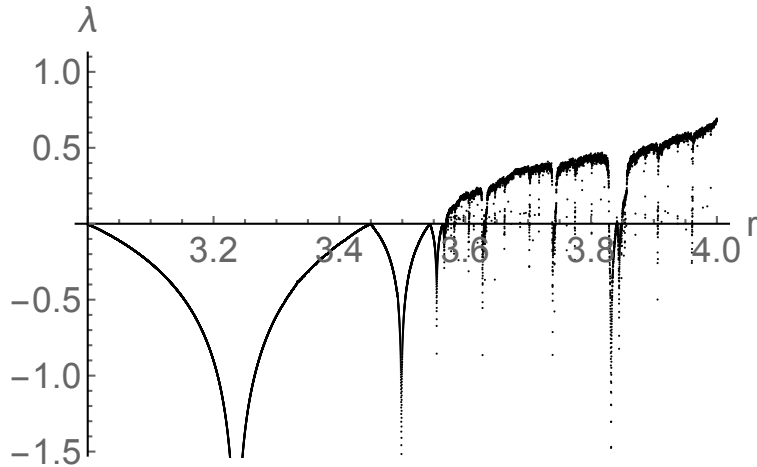


Figure 7.65: Value of the Lyapunov Exponent as a function of  $r$ . The chaotic regimes correspond to  $\lambda > 0$ . (Finite sampling leads to the discrete points.)

You may have noticed that period doubling occurs after progressively shorter intervals as the parameter  $r$  is increased in the case of the logistic map. In fact, for a wide class of maps (and nonlinear differential equations), this speed-up is characterized by a *universal* number. For a parameter  $r$ , denoting  $r_\alpha$  as the value where the  $\alpha^{\text{th}}$  period doubling occurs, then

$$\delta_F = \lim_{\alpha \rightarrow \infty} \frac{r_\alpha - r_{\alpha-1}}{r_{\alpha+1} - r_\alpha} \approx 4.669201 \quad (7.81)$$

is the *Feigenbaum number*. For the logistic map, it is easy to check that we are already pretty close to this number for small  $\alpha$ . Given this, we can estimate where chaos starts as follows:

$$\delta_1 = r_2 - r_1 = \sqrt{6} - 2 \quad \text{and} \quad \delta_n = r_{n+1} - r_n = \frac{\delta_{n-1}}{\delta_F} = \dots = \frac{\delta_1}{\delta_F^{n-1}}, \quad (7.82)$$

so our estimate for where chaos starts is

$$r = \lim_{n \rightarrow \infty} r_n = 3 + \sum_{n=1}^{\infty} \delta_n \simeq 3 + \delta_1 \sum_{n=1}^{\infty} \delta_F^{-(n-1)} = 3 + \frac{\delta_1}{1 - \frac{1}{\delta_F}} = 3.572 \quad (7.83)$$

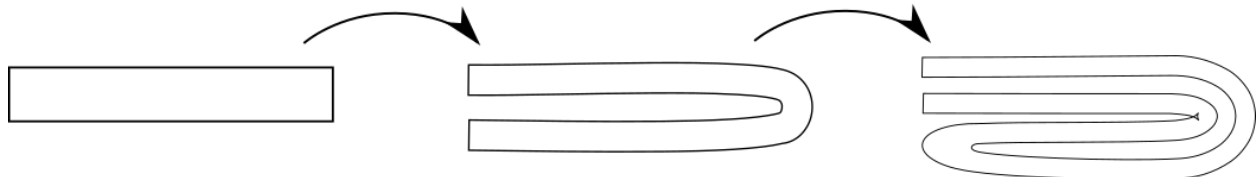
which is fairly close to the real value of  $r = 3.5699456$ .

You may be wondering how trajectories can diverge exponentially (initially) while still remaining bounded. The mechanism is by *stretching and folding* of trajectories. Think of a drop of food coloring on cookie dough which you then fold and knead. To see this more explicitly, lets once again returning to the logistic map in Eq.(7.69), but now we take  $r \simeq 4$ . Then:

$$x_n \in \left(0, \frac{1}{2}\right) \text{ is sent to } x_{n+1} \in (0, 1) \quad (7.84)$$

$$x_n \in \left(\frac{1}{2}, 1\right) \text{ is sent to } x_{n+1} \in (1, 0) \quad (7.85)$$

so the two resulting intervals are the same however in opposite directions. Together the original  $(0, 1)$  interval is both stretched and bent. We then repeat this, with the phase space structure getting progressively more complicated as depicted below:



Finally, there is a self-similarity property of the bifurcation diagram for the logistic map. When we zoom in on regions of smaller scales of  $r$ , we see the same picture again, including the periodic windows, chaotic regions, and period doubling. This is a property of fractals that we'll see shortly.

## 7.6 Chaos in Differential Equations, Strange Attractors, and Fractals

### 7.6.1 The Lorenz Equations

The prototypical example of chaos in differential equations consists of the *Lorenz equations*

$$\begin{cases} \dot{x} = \sigma(y - x) \\ \dot{y} = rx - y - xz \\ \dot{z} = -bz + xy \end{cases} \quad (7.86)$$

where the 3 parameters  $\sigma$ ,  $r$ , and  $b$  are all positive. Note the symmetry under  $x \rightarrow -x$  and  $y \rightarrow -y$ . Lorenz discovered chaotic behavior in his study of atmospheric modeling, which he showed also appeared in these simpler three equations. This serves as a simplified model of a fluid in a convection roll, with  $x$  being the average velocity in the loop,  $y$  being the temperature difference between the flow on the two halves of the roll, and  $z$  being the temperature difference between the inside and outside of the roll. One can think of these equations as an approximation arising from the full Navier-Stokes and heat transfer equations.

The fixed points are  $x^* = y^* = z^* = 0$  which is stable for  $r < 1$  or a saddle point for  $r > 1$ , and  $x^* = y^* = \pm\sqrt{b(r-1)}$  and  $z^* = r-1$  which only exist for  $r > 1$ . At  $r = 1$  there is a supercritical pitchfork bifurcation of the fixed point. With some work, we can show that the  $r > 1$  stable fixed points only remain stable up to  $r = r_H$ , and are unstable beyond that. At this point  $r = r_H$  the stable fixed point prongs each become unstable under subcritical Hopf bifurcations, which involve a collision with an unstable limit cycle that shrinks onto each of the fixed points. This is shown in Fig. 7.66.

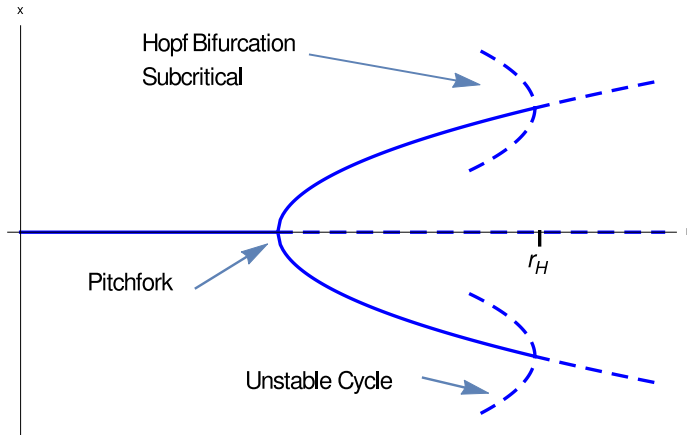


Figure 7.66: Bifurcation Diagram of the  $x$  coordinate of the Lorenz system

We also know that in this system the phase space volumes contract  $\nabla \cdot \vec{f} = -(\sigma+b+1) < 0$  (so the system is dissipative). It can also be shown that trajectories are (eventually) bounded by a sphere  $x^2 + y^2 + (z - r - \sigma)^2 = \text{constant}$ .

In the Lorenz system, for  $r < r_H$  the trajectories converge on a stable fixed point. What happens for  $r > r_H$ ? The trajectories are bounded and the phase space volume shrinks, but there are no stable fixed points or stable limit cycles to serve as attractors. Instead, we have chaos with a *strange attractor*, which is depicted in Fig. 7.67.

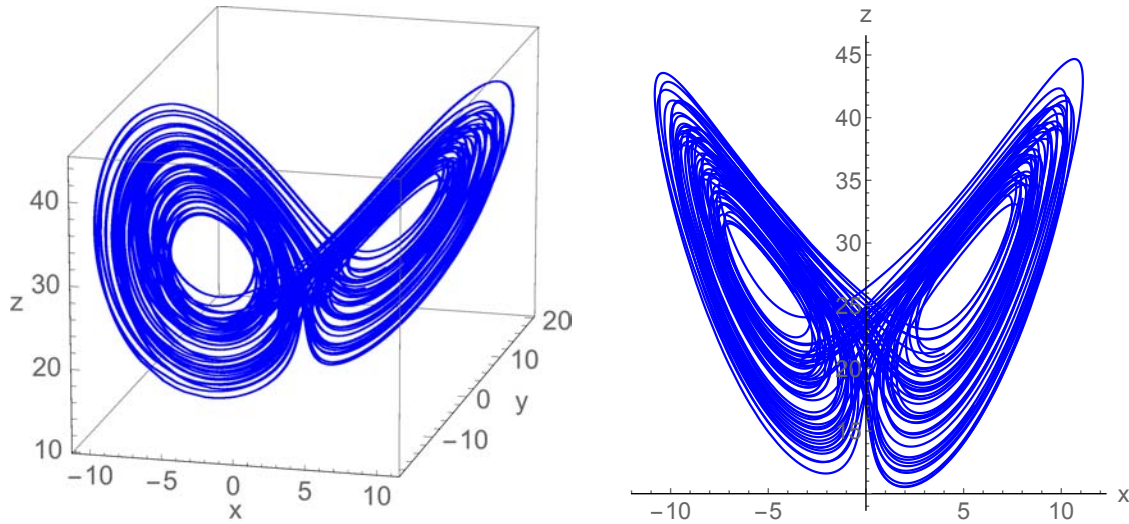


Figure 7.67: Strange attractor in the chaotic regime of the Lorenz equations, shown in the 3-dimensional space as well as for the  $x$ - $z$  projection.

In a strange attractor, the trajectories still never cross (in the 3 dimensions), and the attractor trajectory exhibits *exponential* sensitivity to initial conditions. It also has zero volume consistent with  $\dot{V} = \int \nabla \cdot \vec{f} dV$ , but interestingly, it has infinite surface area! There are infinitely many surfaces traced out by cycles near the fixed points, so the attractor is a *fractal*. For the Lorenz system, surfaces are different after each pass from  $x > 0$  to  $x < 0$  and vice versa; this attractor is a fractal with dimension  $2 < D < 3$ . In fact  $D \simeq 2.05$  in this case.

How can we have exponential divergence of trajectories while the phase space volume shrinks? For the Lorenz system, we have 3 variables, so there are 3 directions in which trajectories can converge or diverge. (In general, these directions are more complicated than simply fixed Cartesian axes. We must find the principal axes at each time.) Thus there are in principle 3 exponents governing the trajectories:

$$\delta_j = \delta_{j0} e^{\lambda_j t} \text{ for } j \in \{1, 2, 3\} \quad \Rightarrow \quad V(t) \approx V_0 e^{(\lambda_1 + \lambda_2 + \lambda_3)t} \quad (7.87)$$

For a case where  $\nabla \cdot \vec{f}$  is constant this means that:

$$\dot{V} = (\lambda_1 + \lambda_2 + \lambda_3)V(t) = \int \nabla \cdot \vec{f} dV = \nabla \cdot \vec{f} V(t) < 0. \quad (7.88)$$

Note that  $\nabla \cdot \vec{f} = -(\sigma + b + 1)$  is constant for the Lorenz system. This means  $\lambda_1 + \lambda_2 + \lambda_3 = \nabla \cdot \vec{f} < 0$ , and the system is dissipative if the sum of the exponents is negative, indicating that the volume shrinks overall. But exponential sensitivity to initial conditions only requires  $\lambda_j > 0$  for at least one value of  $j$ . Here, the *Lyapunov exponent* is defined as  $\lambda \equiv \max(\lambda_1, \lambda_2, \lambda_3)$ .

For the nonlinear damped driven oscillator, we also have  $\lambda_1 + \lambda_2 + \lambda_3 = \nabla \cdot \vec{f} = -\frac{1}{q} < 0$ . Here, things are even simpler because  $\varphi = \omega_D t$  has  $\lambda_3 = 0$ , so  $\lambda_1 + \lambda_2 = -\frac{1}{q}$ . For the undamped case ( $q \rightarrow \infty$ ), we can still have chaos with  $\lambda_1 = -\lambda_2 > 0$ . Thus we note that chaos can occur in both conservative and dissipative systems.

We can think of an area in phase space as it gets stretched and contracted as pictured below. Here it is stretched by the exponent  $\lambda_1 > 0$  and contracted by  $\lambda_2 < 0$ . If trajectories are bounded then it must also get folded.

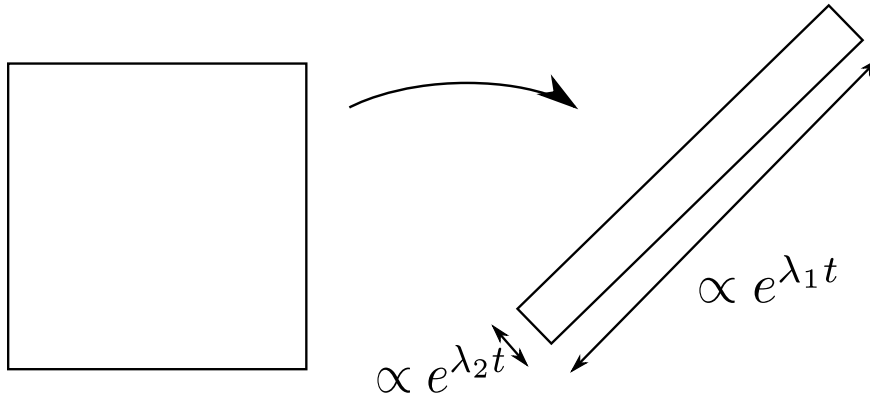


Figure 7.68: The action of the system leads to stretching and rotation of phase space volume.

### 7.6.2 Fractals and the Connection to Lyapunov Exponents

Fractals are characterized by a nontrivial structure at arbitrarily small length scales. In particular, they are self-similar (in that they contain copies of themselves at arbitrarily small scales).

**Example:** The Cantor set fractal is created by iteratively removing the middle  $\frac{1}{3}$  of a line segment. If  $S_0$  is the line segment  $0 \leq x \leq 1$ , then  $S_1$  is formed by removing the middle  $\frac{1}{3}$  of  $S_0$ ,  $S_2$  is formed by removing the middle  $\frac{1}{3}$  of each piece of  $S_1$ , and so on until the true Cantor set emerges as  $S_\infty$ . This is pictured in Fig. 7.69. Here the number of separate pieces grows infinitely large (and is in fact non-denumerable), while the total length of the pieces

tends to zero. (This is the one dimensional analog of area  $\rightarrow \infty$  with volume  $\rightarrow 0$  for the Lorentz equations strange attractor.) The Cantor set also has the self-similar property.



Figure 7.69: Illustration of the iterative procedure that produces the Cantor Set.

How do we define a non-integer dimension for fractals? Let us consider covering a line of length  $a_0$  with segments of length  $a$ . We would need  $N(a) = \frac{a_0}{a}$  segments. For a square of side length  $a_0$  covered by smaller squares of side length  $a$ , we would need  $N(a) = \left(\frac{a_0}{a}\right)^2$  squares. In general, for a  $D$ -dimensional hypercube of side length  $a_0$  covered by  $D$ -dimensional hypercubes of side length  $a$ , we would need  $N(a) = \left(\frac{a_0}{a}\right)^D$  such hypercubes for integer  $D$ . This can be generalized beyond integers to

$$d_F = \lim_{a \rightarrow 0} \frac{\ln(N(a))}{\ln\left(\frac{a_0}{a}\right)} \quad (7.89)$$

which is the *Hausdorff dimension* (also called the capacity dimension or the fractal dimension).

**Example:** in the Cantor set, after  $n$  steps, the number of segments is:

$$N(a) = 2^n \quad (7.90)$$

while the length of each segment goes as:

$$a_n = \frac{a_0}{3^n} \quad (7.91)$$

Thus the fractal dimension is given by:

$$d_F = \lim_{n \rightarrow \infty} \frac{\ln(2^n)}{\ln(3^n)} = \frac{\ln(2)}{\ln(3)} \simeq 0.6309 \quad (7.92)$$

indicating that it is less than a line with  $d_F = 1$  but more than a point with  $d_F = 0$ .

In general, fractal dimensions are not integers and are usually irrational.

**Example:** The Koch curve is like the Cantor set, except that instead of deleting the middle  $\frac{1}{3}$  of every segment, we replace it by an equilateral triangle on the other two sides, so segments are overall added rather than removed. The Koch curve corresponds to one of the sides of the Koch Snowflake depicted below in Fig. 7.70. In this case:

$$N(a) = 4^n \quad \text{and} \quad a_n = \frac{a_0}{3^n} \quad \Rightarrow \quad d_F = \frac{\ln(4)}{\ln(3)} \simeq 1.262 \quad (7.93)$$

which satisfies  $1 < d_F < 2$ . This means the Koch curve has infinite length (1-dimensional volume) but zero area (2-dimensional volume).

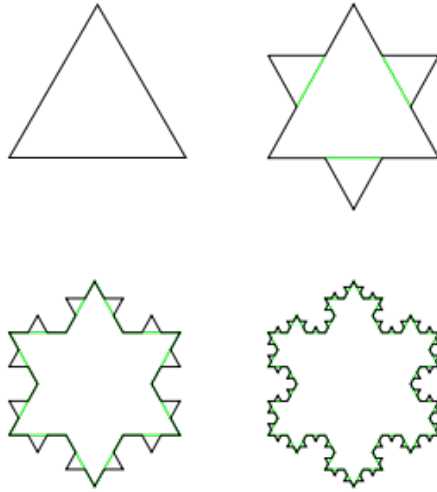


Figure 7.70: The Koch Curve corresponds to starting with just one of the 3 sides of the triangle used to generate the Koch Snowflake shown here.

We can connect the notion of a fractal dimension to Lyapunov exponents which govern the behavior of physical trajectories. For simplicity, let us consider an example with  $\lambda_1 > 0$ ,  $\lambda_2 < 0$ , and  $\lambda_3 = 0$ . The area of a square of phase space points evolves as:

$$A(t=0) = a_0^2 \rightarrow A_0(t) = a_0^2 e^{(\lambda_1 + \lambda_2)t} \quad (7.94)$$

while the squares covering it have area  $A(t) = a_0^2 e^{2\lambda_2 t}$ , see Fig. 7.71. Therefore

$$N(t) = \frac{A_0(t)}{A(t)} = e^{(\lambda_1 - \lambda_2)t} \quad (7.95)$$

This gives rise to a fractal dimension of:

$$d_F = 1 + \frac{\lambda_1}{|\lambda_2|} \quad (7.96)$$

which is the *Kaplan-Yorke relation*. A fixed point attractor has  $d_F = 0$ , and a limit cycle attractor has  $d_F = 1$ . By contrast, a strange attractor generally has a non-integer  $d_F$ , and this dimension is related to the sensitivity to initial conditions (given by  $\lambda_1$ ) as well as to the contraction of phase space (given by  $\lambda_2$ ).

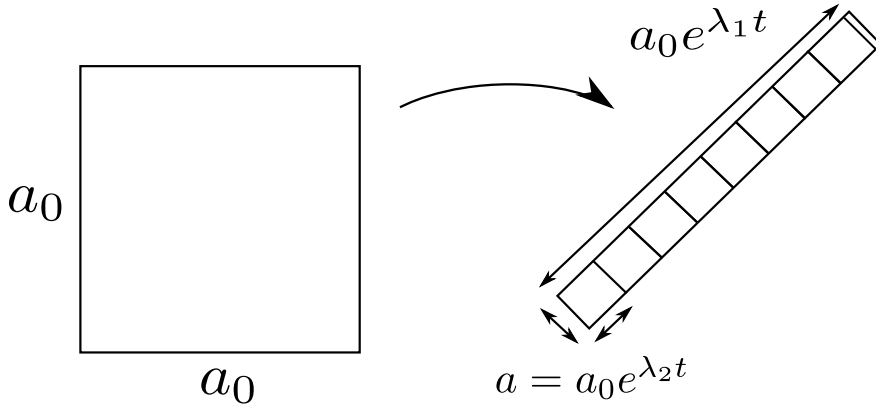


Figure 7.71: As the system evolves the phase space volume changes, so our tiling volume changes as well.

### 7.6.3 Chaos in Fluids

Chaos can occur in fluids as well. If we take  $\nabla \cdot \mathbf{v} = 0$  and  $\rho$  to be constant and uniform, the Navier-Stokes equation says:

$$\frac{\partial \mathbf{v}}{\partial t} = -\mathbf{v} \cdot \nabla \mathbf{v} - \frac{\nabla P}{\rho} + \nu \nabla^2 \mathbf{v} \quad (7.97)$$

and this should be used in conjunction with the heat transfer equation. In the language we have been using in this chapter, the velocity field  $\mathbf{v}(\mathbf{x}, t)$  corresponds to a continuum of variables (each labeled by  $\mathbf{x}$ ). One can also think of the terms involving  $\nabla \mathbf{v}$  as couplings between these variables, like finite differences, for example:

$$\frac{\partial v_x}{\partial x} \approx \frac{v_x(x + \epsilon) - v_x(x - \epsilon)}{2\epsilon} \quad (7.98)$$

In some cases (as in convection rolls per the Lorenz equations), we can have aperiodic time dependence but spatial regularity in  $\mathbf{x}$ . Here, many of the ideas that we have studied (like, for example, the period doubling road to chaos) apply. In other cases, the spatial structure in  $\mathbf{x}$  also becomes irregular. The regularity (or lack thereof) can also depend on initial conditions. This happens, for example, in fat convection rolls in shallow fluids. Essentially there could be multiple attractors present. For the case with irregularity in  $\mathbf{x}$ , the dimensionality of the attractor is proportional to the size of the system, which is very large! Here it makes more sense to speak of a “dimension density”.

Strong turbulence in a fluid falls in the category of being irregular in  $\mathbf{x}$  with no characteristic size for features. This is certainly more advanced than our examples, and indeed a full formalism for turbulence remains to be invented. One thing we can do to characterize strong turbulence is apply dimensional analysis.

There are several scaling laws for turbulence in 3 dimensions. Recall that vortices (eddies) appear at all length scales  $\lambda$  and are efficient at transferring energy. Let us define  $L$  as the size of the fluid container,  $\lambda_0$  as the scale where dissipation is important (for Reynolds number  $R \approx 1$ ),  $\epsilon$  as the mean energy transfer per unit time per unit mass, and  $v_\lambda$  as the velocity variation at length scale  $\lambda$ . Note that the dimensions  $[\nu] = m^2/s$  and  $[\epsilon] = (kgm^2/s^2)(1/skg) = m^2/s^3$ . There are three scales to consider.

1. At  $\lambda \approx L$ , there can be no dependence on  $\nu$ , so  $\epsilon \propto \frac{v_L^3}{L}$ . (This is the scale with the most kinetic energy and the largest energy.)
2. At  $\lambda_0 \ll \lambda \ll L$ , there can still be no  $\nu$ , so here  $\epsilon \propto \frac{v_\lambda^3}{\lambda}$ . Note that this is independent of the properties  $\rho$ ,  $\nu$  and the scale  $L$  of the fluid!
3. At  $\lambda \approx \lambda_0$ , because  $R = \frac{v_0 \lambda_0}{\nu} \approx 1$ , then  $v_0 \approx \frac{\nu}{\lambda_0}$ . This is where the energy dissipation occurs. Here we only have  $\nu$  and  $\lambda_0$  present, so  $\epsilon \propto \frac{\nu^3}{\lambda_0^4}$ .

Rather than using  $\lambda$  and  $v_\lambda$ , the universal result for the case  $\lambda_0 \ll \lambda \ll L$  is often written in terms of the wavenumber  $k \propto \frac{1}{\lambda}$  and kinetic energy per unit mass per unit wave number,  $E(k)$ . The kinetic energy per unit mass can be written as  $E(k) dk$ . Here  $E(k)$  behaves as a rescaled version of the energy with slightly different dimensions,  $[E(k)] = m^3/s^2$ . Analyzing its dimensions in relation to  $\epsilon$  and  $k$  we note that  $m^3/s^2 = (m^2/s^3)^{2/3}(1/m)^{-5/3}$  which yields

$$E(k) \sim \epsilon^{\frac{2}{3}} k^{-\frac{5}{3}} \quad (7.99)$$

This is the famous Kolmogorov scaling law for strong turbulence. It provides a mechanism by which we can make measurements and probe a universal property of turbulence in many systems.

The End.

MIT OpenCourseWare  
<https://ocw.mit.edu>

**8.09 Classical Mechanics III**

Fall 2014

For information about citing these materials or our Terms of Use, visit: <https://ocw.mit.edu/terms>.